Available online at www.sciencedirect.com

ScienceDirect

Geochimica et Cosmochimica Acta 285 (2020) 237–256

Geochimica et Cosmochimica Acta

www.elsevier.com/locate/gca

Drip water $\delta^{18}O$ variability in the northeastern Yucatán Peninsula, Mexico: Implications for tropical cyclone detection and rainfall reconstruction from speleothems

Fernanda Lases-Hernández [a,*], Martín Medina-Elizalde [b,1], Amy Benoit Frappier [c]

[a] Centro de Geociencias, UNAM Campus Juriquilla, Blvd. Juriquilla 3001, Juriquilla, Querétaro 76230, Mexico
[b] Department of Geosciences, Auburn University, AL, United States[2]
[c] Department of Geosciences, Skidmore College, Saratoga Springs, NY 12866, United States

Received 10 February 2020; accepted in revised form 5 July 2020; available online 14 July 2020

Abstract

This study examines the oxygen isotopic composition ($\delta^{18}O$ values) of drip water, rainfall, and groundwater in the Río Secreto cave system, located in the Yucatán Peninsula, Mexico. The main motivation of this study was to determine the implications of drip water hydrology for the reconstruction of rainfall, droughts and tropical cyclone activity from stalagmite $\delta^{18}O$ records. Monitoring of environmental and isotopic conditions was conducted for two years, from June 2017 to April 2019. This study provides the first instrumental evidence of an "amount effect" on interannual timescales in the Yucatán Peninsula. Observed bi-weekly to interannual variability in drip water $\delta^{18}O$ values can be explained for individual drips by different integrations of rainfall amount in the time domain. Drip sites in two chambers (Stations A and B) integrate 4–15 months of rainfall accumulation. In a third chamber (Station LF) one drip site reflects the annual rainfall isotopic cycle with a positive offset and another, the largest rainfall events. During epikarst infiltration, the integration of rainfall amount by drip water source reservoirs determines the degree to which they "dilute" a tropical cyclone (TC) isotopic signature. TCs can be detected particularly when: (1) the water volume of the reservoir is low, such as during a persistent meteorological drought, and; (2) TCs have a sufficiently distinct isotopic signal relative to that of the reservoir prior to the event. TC isotopic signals can be masked or attenuated when drip water samples integrate more than a week and if significant rainfall events proceed the TC. In Río Secreto cave, reconstructing precipitation amount and detecting the TC isotopic signatures from stalagmite $\delta^{18}O$ records is possible. Our analysis shows that stalagmite $\delta^{18}O$ records are more likely to underestimate the magnitude of annual-scale droughts following normal hydroclimate conditions and more likely to record TCs during multiyear droughts than during normal or wet periods. Drip water monitoring results suggest that available stalagmite $\delta^{18}O$ records from the Maya lowlands might be underestimating the intensity of paleo-drought events, such as the Terminal Classic droughts associated with the disintegration of the Maya civilization. This study complements the results from Lases-Hernandez et al. (2019) comparing two different sampling protocols of drip water collection. This study shows that a discrete sampling protocol is expected to approximate the amount-weighted isotopic composition of a drip, as long as it is conducted at a temporal resolution higher

* Corresponding author.
E-mail addresses: flases@geociencias.unam.mx (F. Lases-Hernández), martin.medina@auburn.edu (M. Medina-Elizalde), afrappie@skidmore.edu (A. Benoit Frappier).
[1] From August 16, 2020: Department of Geosciences, UMASS, Amherst, United States.
.

https://doi.org/10.1016/j.gca.2020.07.008

than the rainfall integration time by the drip reservoir. We highlight the importance of conducting multiyear monitoring of drip water and rainfall in order to interpret stalagmite $\delta^{18}O$ as a paleoclimate proxy.

Keywords: Speleothem; Tropical cyclones; Vadose; Hydrology; Drought; Stalagmite; Oxygen isotopes

1. INTRODUCTION

The frequency and intensity of precipitation extremes are expected to increase globally as human greenhouse gas emissions (GHG) continue to rise over the 21st century (Huntington, 2006; Williams et al., 2007; Déry et al., 2009; O'Gorman and Schneider, 2009; Lu and Fu, 2010; Seager et al., 2010; Wu et al., 2010; Kao and Ganguly, 2011; Müller et al., 2011; Durack et al., 2012). Intergovernmental Panel of Climate Change (IPCC-AR5) projections of precipitation variability in response to GHG forcing over the 21st century show large uncertainties, particularly in regions between tropical and subtropical climates. Paleoclimate studies have the potential to help reduce these uncertainties by providing empirical estimates of precipitation responses to shifts in internal modes of climate variability and the atmospheric composition of GHGs.

Stalagmite calcite or aragonite oxygen isotope ($\delta^{18}O$ value) records represent one of the most promising terrestrial paleoclimate archives with the potential to yield semi-quantitative records of precipitation variability and records of tropical cyclone (TC) activity in tropical and subtropical regions (e.g. Wang et al., 2001; Frappier et al., 2007a; Fleitmann et al., 2009; Medina-Elizalde et al. 2010; Kennett et al., 2012; Partin et al, 2012; Akers et al., 2016; Baldini et al., 2016; Medina-Elizalde et al., 2017).

In these regions, stalagmite $\delta^{18}O$ records have been interpreted either explicitly or implicitly to reflect the "amount effect"; that is, the inverse relationship between rainfall amount and rainfall $\delta^{18}O$ described by Dansgaard (1964), that occurs on seasonal and interannual time scales in low and mid-latitude regions (Vuille et al., 2003; Lachniet and Patterson, 2009; Medina-Elizalde et al. 2016a; Lases-Hernandez et al., 2019). The working hypothesis of stalagmite hydrological records from these regions is often that calcite and aragonite deposited under isotopic equilibrium conditions preserve the rainfall $\delta^{18}O$ composition thus recording rainfall amount (Burns et al., 2003; Medina-Elizalde et al., 2010). This approach assumes that other potential effects on rainfall $\delta^{18}O$ within these regions may be negligible such as temperature, evaporation, source moisture $\delta^{18}O$ and plant transpiration (Fairchild and Treble, 2009; Wang et al., 2017; Wang et al., 2001).

Although seldom acknowledged in studies of paleohydrological records based on stalagmites, the isotopic relationship between rainfall and drip water is crucial when comparing relative isotopic variations within a single stalagmite and among different stalagmite $\delta^{18}O$ records, and particularly if the goal is to reconstruct precipitation amount quantitatively (e.g. Medina-Elizalde et al., 2010; Lachniet et al., 2012, 2017; Medina-Elizalde and Rohling, 2012; Aharon and Dhungana, 2017; Medina-Elizalde et al., 2017). The $\delta^{18}O$ signature of rainfall may be altered between the ground surface and the cave interior due to processes including isotopic fractionation in the soil, epikarst and/or vadose zone, driven by evaporation (Ayalon et al. 1998; Bradley et al. 2010; Cuthbert et al., 2014; Beddows et al. 2016, Hartmann and Baker, 2017), and by mixing with other meteoric water reservoirs in the epikarst, which essentially attenuates the isotopic signal of a rainfall event (Yonge et al., 1985; Ayalon et al., 1998; Williams and Fowler, 2002; McDermott, 2004; Fairchild et al., 2006; Lachniet and Patterson, 2009; Genty et al., 2014; Hartmann and Baker, 2017). The resolution of a stalagmite $\delta^{18}O$-derived rainfall record, importantly, is not determined solely by the stalagmite sampling resolution, but also by the time integration of the rainfall signal during drip water infiltration (Lases-Hernandez et al., 2019). Drip-specific infiltration pathways can potentially integrate the amount-weighted isotopic signal of rainfall accumulated over days (Luo et al. 2014, Duan et al. 2016), a season (Cruz, 2005; Cobb et al., 2007; Fuller et al., 2008; Genty, 2008; Beddows et al. 2016; Duan et al. 2016), a year or even multiple years (Yonge et al., 1985; Williams and Fowler, 2002; Onac et al., 2008; Genty et al., 2014; Riechelmann et al., 2011, 2017; Czuppon et al., 2018; Jean-Baptiste et al., 2019). Moreover, the drip sites within a single cave can exhibit different responses to the same isotopic signal of the rainfall infiltrating water (Treble et al., 2013; Moerman et al. 2014; Pérez-Mejías et al. 2018; Lases-Hernandez et al., 2019).

Drip water isotopic information, therefore, is critical to validate studies with high-resolution stalagmite $\delta^{18}O$ records that seek to characterize seasonal to interannual precipitation variability (Medina-Elizalde et al. 2010, Medina-Elizalde and Rohling, 2012; Kennett et al. 2012, Lachniet et al., 2012, 2017) or to discern the negative isotopic anomalies of TC rainfall (Frappier et al., 2007a; Baldini et al. 2016).

The present study presents new drip water isotopic data from drip sites monitored from June 2017 to April 2019 in the Río Secreto cave system, located in the northeastern coast of the Yucatán Peninsula (YP), Mexico (Fig. 1). These drip sites are 7 of the 16 previously examined by Lases-Hernandez et al. (2019) (hereafter LH19), and were selected because they represent distinctive isotopic patterns with variable implications for paleoclimate reconstruction. In this study we applied a new sampling protocol different from that of LH19 which: (i) enabled the characterization of all the water discharged at these 7 drip sites over two years; (ii) help test the influence of LH19's sampling protocol on a positive isotopic bias observed at a drip site with a small reservoir size (labelled LF1) (details in Section 2.2);

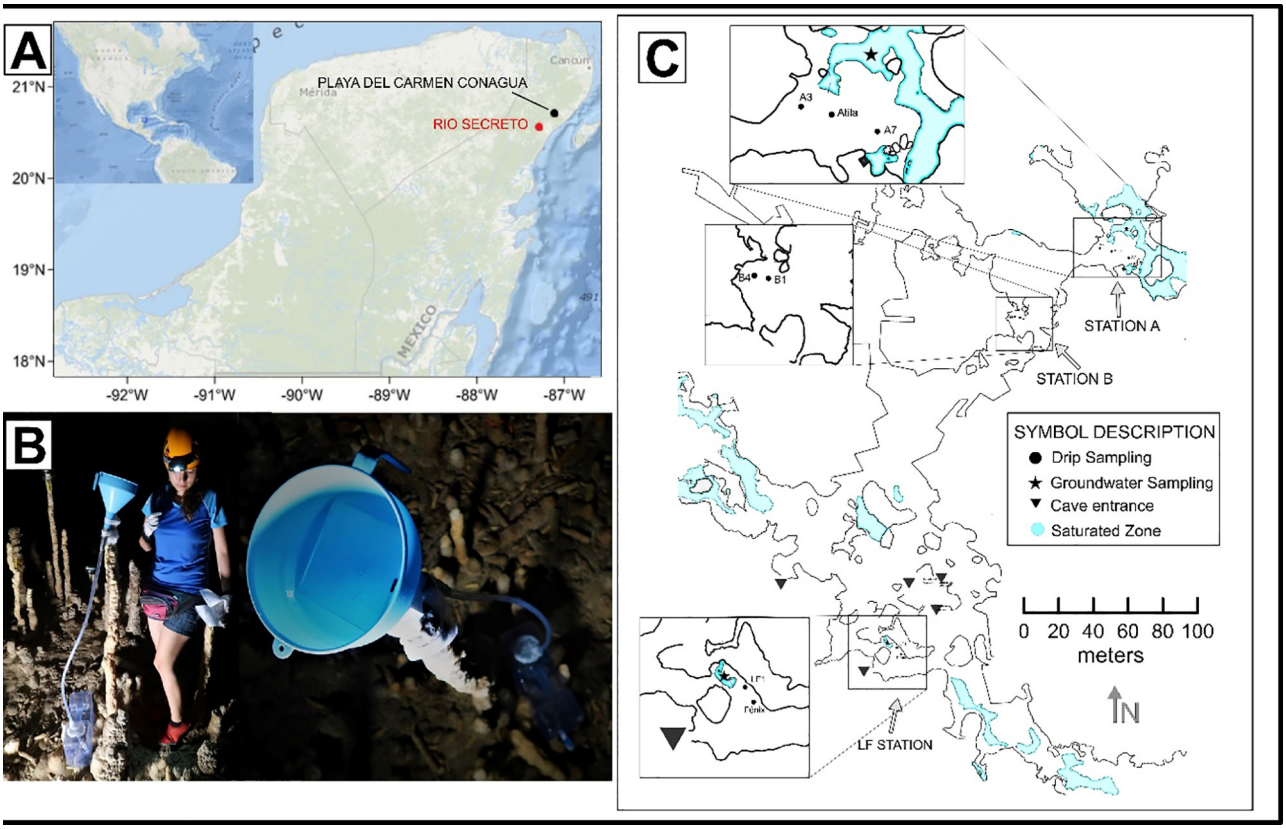

Fig. 1. (A) Location of Río Secreto cave (red dot) and weather station of Playa del Carmen (CONAGUA) (black dot). (B) Example of collection of drip water system at A7 drip site, visible also is a glass plate inside the funnel used to farm calcite (See Section 3.2). (C) Map of the monitored stations A, B and LF (modified from Sprouse et al. 2017). (For interpretation of the references to colour in this figure legend, the reader is referred to the web version of this article.)

(iii) enabled estimates of rainfall integration times and degree of homogenization, stratified by reservoir, of six of these seven drip sites, from bi-weekly, monthly and annual drip water samples, and; (iv) help test the notion that the isotopic composition of drip water at different drip sites converge into a single value when drip water is integrated over a sufficiently long period and provided they reflect the same water source and no other process, such as evaporation, has altered the isotopic composition of the water source. In addition, this study explores the implications of observed drip water variability and residence times for the detection of significant precipitation reductions (i.e. droughts) and TCs from stalagmite $\delta^{18}O$ records. Lastly, we provide the first instrumental evidence of the existence of a rainfall *amount effect* on interannual timescales for the YP.

2. FIELD SITE

2.1. Study site, cave system and climate

The annual precipitation cycle in the YP is recognized to have three distinctive seasons known as Dry, Rainy and Nortes. The *Dry* season corresponds to the months from March to May when the region experiences the lowest amount of precipitation in the course of the year. The *Rainy* season, concurrent with the so-called "hurricane season", has a bimodal distribution of precipitation with precipitation peaks in June and September and a midsummer drought, or *Canícula,* during July and August (Magaña et al., 1999). During the *Rainy* season the Intertropical Convergence Zone (ITCZ) and its belt of convective activity reach their northernmost position producing peak precipitation in the month of September coeval with maximum tropical cyclone frequency affecting the YP. The *Nortes* season happens during the months of November and February and is characterized by the influence of northern cold fronts which bring cold weather and isotopically distinctive rainfall into the YP.

The Río Secreto ("Secret River") cave is a semi-flooded karst system located in the northeast of the YP in the State of Quintana Roo, Mexico (20° 35.244'N; 87° 8.042'W, Fig. 1). The karst cave system is mostly horizontally developed and with an extension larger than 42 km surveyed by Sprouse et al. (2017). The cave is 5 km south of the city of Playa del Carmen, and the main entrance is five km from the Caribbean coast. Río Secreto cave has been used for tourism purposes since the year 2008, although only about 10% of the cave is used for this purpose. Río Secreto cave is located less than 10 km away from the CONAGUA (National Water Office) meteorological station located in Playa del Carmen city. Average annual precipitation in

Playa del Carmen is 1390 ± 280 mm (14-year monthly averages 1998–2011; Table E in Supplementary Material). More than 70% of total annual precipitation occurs during the *Rainy* season from June to November and therefore recharge is also biased to the these months (Medina-Elizalde et al., 2016b; Lases-Hernandez et al., 2019).

The bedrock at Río Secreto cave is composed by Pliocene-Pleistocene carbonates that retain much of its primary porosity, although infiltration is given mostly through small fractures and secondary porosity features. The vadose zone of Río Secreto cave and of most caves in the northeastern YP is within the epikarst and the bedrock thickness is from 2 to 12 m (Lases-Hernandez et al., 2019). The water table in Rio Secreto is located ~15 m from the surface and has a very low hydraulic gradient in the range of 10^{-5} cm per km (Bauer-Gottwein et al., 2011). Río Secreto cave has several sinkholes with a diameter from 1 to 8 meters that allow access to the cave and its ventilation. The overlaying soil is very thin and heterogeneous, with soil pockets < 0.5 m deep between frequent areas of exposed bedrock (Lases-Hernandez et al., 2019).

2.2. Previous study in the Río Secreto cave system

LH19 determined the isotopic composition of drip water, groundwater, and rainfall from three different chambers within the Rio Secreto cave system. These chambers were labeled Station Laberinto del Fauno (LF) and Stations A and B. Monitoring of environmental conditions inside and outside the cave included the measurement of air temperature and relative humidity as well as drip water and groundwater temperatures from 2012 to 2017. Stations A and B are isolated and characterized by having constant temperatures similar to the annual average air temperature outside (~24.5 °C). Station LF presents more variable annual variability of groundwater and air temperature (total range of ~3 °C and ~6 °C, respectively) and air temperature coupled with temperature variability outside. Buoyancy-driven ventilation occurring mainly during winter season produces seasonal temperature variability inside these chambers with a larger effect on the most exposed chamber, the Station LF, as expected (LH19). Relative humidity at Stations A and LF was near to 100% during the 2014–2017 period.

LH19 characterized the oxygen isotopic composition at 16 cave drip sites from these three chambers and results showed that drip sites modulated the amplitude of rainfall $\delta^{18}O$ variability to different degrees. The study by LH19 did not estimate quantitatively the time-integration of rainfall amount by each drip water reservoir, as presented in this current study. At all drip sites (with the exception of drip site labelled Fénix) drip water isotopic compositions were between two end members: (1) drip waters whose annual mean $\delta^{18}O$ values were close to the annual amount-weighted $\delta^{18}O$ composition of rainfall (e.g. drip sites labelled A3, A7, Atila, B1, B4), and; (2) drip waters whose annual mean $\delta^{18}O$ values were close to the arithmetic annual average isotopic composition of rainfall (e.g. LF1). LH19 showed that drip waters whose $\delta^{18}O$ values resemble the annual amount-weighted $\delta^{18}O$ composition of rainfall also presented low intra annual isotopic variability, concluding that they reflect a water reservoir big enough to accumulate rainfall during several months with physical homogenization controlling the water isotope signature over this timescale. Conversely, a small reservoir was inferred for a drip site whose annual mean water $\delta^{18}O$ values was close to the arithmetic annual average isotopic composition of rainfall (e.g. LF1), and that best tracks the $\delta^{18}O$ variability of individual rainfall events. LH19 proposed that these results reflected the sampling protocol consisting of a bi-weekly collection of discrete drip water samples accummulated over 48 hours. According to this hypothesis, the annual average $\delta^{18}O$ composition of drip water would be close to the annual amount-weighted $\delta^{18}O$ composition of rainfall when their reservoirs were large, and close to the unweighted annual average $\delta^{18}O$ composition of rainfall when their reservoirs were small (Fig. 5 in LH19). This is because a large reservoir already integrates the cumulative isotopic signal of many rainfall events and therefore a discrete sample would reflect such temporal integration. In contrast, a small reservoir implies that a discrete sample represents only few rainfall events and an annual isotopic average based on discrete samples would therefore be biased; just like an annual average isotopic composition of rainfall, that does not weigh the amount of individual rainfall events, would be biased relative to the annual amount-weighted isotopic composition of rainfall (Fig. 5 in LH19). This hypothesis was supported by evidence that evaporation, a factor that can also potentially shift LF1 $\delta^{18}O$ positively, was likely negligible, as suggested by: (i) drip water isotopic values similar to the coeval local meteoric water line; (ii) the isotopic composition of drip water at various drip sites similar to that of rainfall; (iii) drip water mean annual $\delta^{18}O$ compositions from Stations A and B closely resembling the annual amount-weighted $\delta^{18}O$ composition of rainfall; (iv) drip water average $\delta^{18}O$ composition from drip site labelled Fénix 1–2‰ more negative than the annual amount-weighted $\delta^{18}O$ composition of rainfall, and; (v) cave air relative humidity at or near 100% during the entire recorded period.

One motivation of this work is to test whether the positive isotopic offset of drip site LF1 relative to the annual amount-weighted $\delta^{18}O$ composition of rainfall reflects an artifact of the discrete sample protocol, by adopting a continuous sampling method. We note that if the positive isotopic bias of LF1 were a reflection of the sampling protocol and not evaporation, a stalagmite from this drip would be ideal to identify the short-lived fluxes from TCs.

The drip site labelled Fénix, located ~ 5 m from LF1, presented a conondrum as it showed the lowest variability and the most depleted isotopic values of the 16 drip sites investigated. Fénix's drip rates suggested a discharge flow coeval with seasonal rainfall amount changes, but its $\delta^{18}O$ values showed negligible variability (<0.4 ‰) and an isotopic composition 1 to 2‰ more depleted than the annual amount-weighted $\delta^{18}O$ composition of rainfall. To explain Fénix's lack of isotopic variability and negatively biased isotopic composition, LH19 hypothesized that the epikarst above Fénix was thin enough to allow primarly infiltration of large rainfall events with their associated depleted $\delta^{18}O$

values resulting from an *amount effect*. Due to Fénix's very large reservoir, on the other hand, these rainfall events did not have enough volume to modify significantly the reservoir's isotopic signature, thus explaining its characteristic low isotopic variability over time. In this study we continued monitoring Fénix in order to better understand its long-term response to rainfall $\delta^{18}O$ variability, particularly during times of drought.

Lastly, LH19 document that drip discharge typically lagged rainfall amount shifts by few weeks and up to three months. According to the methodology of Fairchild et al. (2006), the drip sites we monitor in this study, A3, A7, B4 and Fénix are drips that maintain a high and temporally constant drip rate seasonally and are thus classified as "Seepage flow". The other three drip sites we monitor, Atila, B1 and LF1, exhibit higher discharge variability thus corresponding to "Seasonal Drips" (Fig. 7 in LH19).

3. METHODS

3.1. Rainfall sampling

Thirty five rainfall samples were collected between July 2017 and April 2019, using two HDPE 8-liter containers with a connected funnel that had a Ping-Pong ball in it to help prevent potential isotope exchange and water loss from the containers through evaporation, following previous protocols (Lases-Hernandez et al., 2019). Rainfall samples include 22 that integrate 9–59 days labeled "monthly rainfall" and 13 samples that integrate 1–41 days labeled "partial rainfall" (Fig. 2). Sample periods of rainfall accumulation are presented in the Supplementary Table A. In addition to rainfall amount data collected at the Río Secreto Nature Reserve, we present coeval rainfall amount data recorded by a meteorological station in the city of

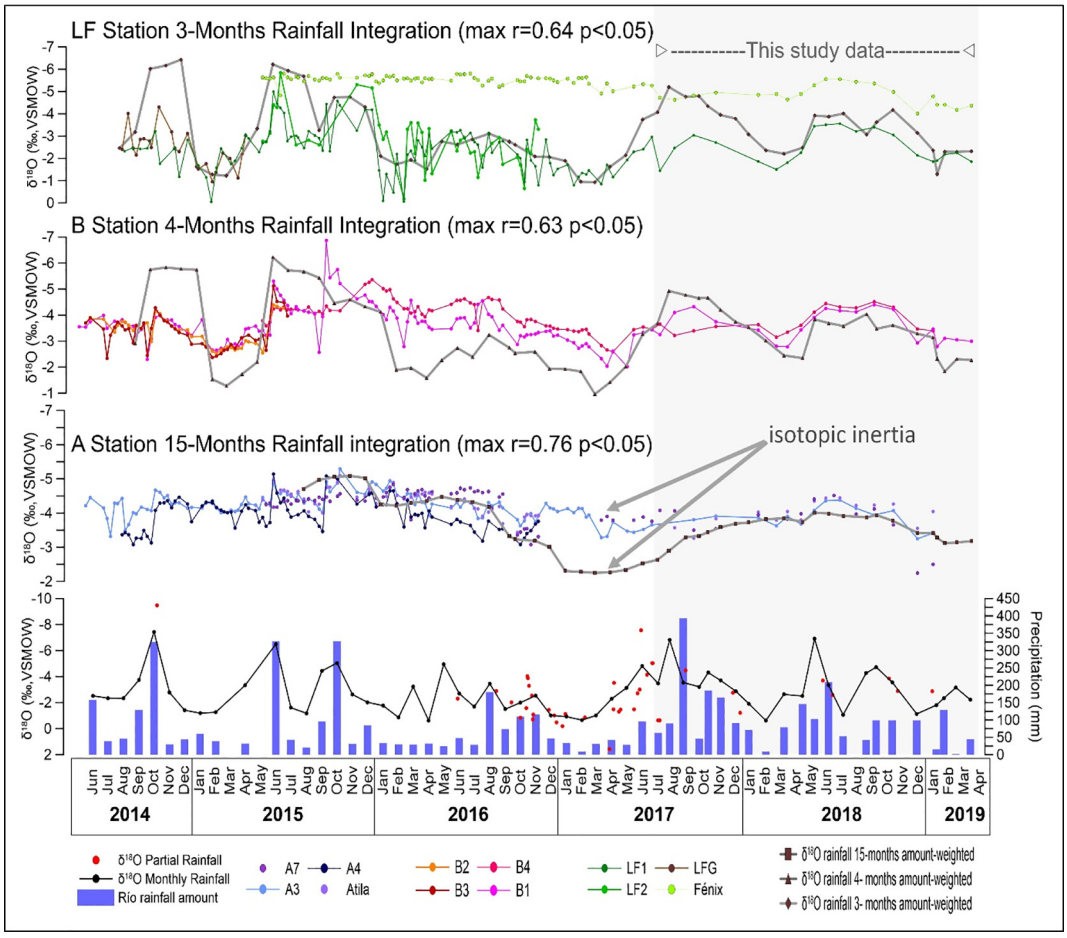

Fig. 2. Upper three panels: drip water $\delta^{18}O$ time series from June 2014 to April 2019 from stations LF, B and A. Superimposed; time series of rainfall amount-weighted $\delta^{18}O$ values integrated over specific time intervals for each station (black lines) (See Sections 3.3.2, 4.4 and 5.2; Supplementary Fig. B and Table G). Lower panel: Rio Secreto rainfall $\delta^{18}O$ composition of monthly samples (black line) and discrete rainfall events (red dots), and rainfall amount (blue rectangles) (See Section 3.1). Note that all the $\delta^{18}O$ axis values are inverted and represent different value ranges. Data before July 2017 are from Lases-Hernandez et al. (2019). (For interpretation of the references to colour in this figure legend, the reader is referred to the web version of this article.)

Playa del Carmen, located 4 Km away from Río Secreto (20°37.200′0N, 87° 04.200′0W). This additional rainfall data offers a broader perspective of spatial variability in this region (Supplementary Table A).

3.2. Drip water and groundwater sampling

Río Secreto Cave drip water $\delta^{18}O$ and discharge rate variability were previously characterized on a ~ bi-weekly basis from monitoring 16 stalactites in three different chambers by LH19 (see Section 2.2). In this study, we selected and monitored 7 of these 16 drip sites, that best represent the types of isotopic variability patterns previously described. Specifically for this study, drip water was collected from two stalactites labeled LF1 and Fénix (located in Station LF), three stalactites labeled A3, A7 and Atila (Station A), and 2 stalactites labeled B1 and B4 (Station B) (Fig. 1). Drip water samples from these 7 stalactites represent 3 to 61 days of water accumulation over the same 22-month period that rainfall water data was collected (Table B Supplemental material).

Drip water from each drip site was collected using a plastic funnel connected with a hose to an HDPE 8-liter container. Connections were sealed following each collection using three layers of Parafilm and one layer of silver tape to avoid evaporation and isotope exchange with ambient water vapor. After water accumulated in the container, one drip water aliquot was taken into a 30 mL Nalgene bottle through the container's spigot to avoid interaction between water and air during sample transfer. Before deployment of the water collection system, all its plastic components were washed with a 10% solution of ultra clean HNO_3, rinsed three times with deionized water, and finally thoroughly dried. After each sample aliquot was collected the total water volume in the collector was quantified using a graduated cylinder. The collection system was fully cleaned and dried as described above, before being reinstalled to collect a new drip water sample. Nitrile gloves were used to manipulate components during sampling work. We point out that within the funnels we placed 10 x10 cm frosted glass plates in order to farm calcite. Glass plates were previously washed with a 10% solution of ultraclean HNO_3 and rinsed three times with deionized water (See video of collection system in Supplementary material). During the visits to the cave, discrete groundwater samples from Stations LF and A were also collected directly from cave pools, 30 cm from the surface, using 30 mL Nalgene bottles (Fig. 1), the dates of sampling can be found in Table E. The isotopic results of farmed calcite will be reported in a subsequent manuscript.

3.3. Analytical methods and Data Interpretation

3.3.1. Stable isotope composition

The $\delta^{18}O$ and δD composition of groundwater, meteoric precipitation and drip water samples were determined using a Cavity Ring-Down Spectroscopy (CRDS) Picarro Isotope Analyzer, model L2130-i at Auburn University, Alabama. Long-term reproducibility of in-house Picarro "Zero" and "Mid" standard waters measurements were better than 0.03 ‰ for $\delta^{18}O$ and at 0.2 ‰ for δD. Results are reported in per mil (‰) relative to VSMOW (Vienna Standard Mean Ocean Water).

3.3.2. Integration of rainfall amount by drip water

In order to determine how much time of rainfall accumulation the drips integrate (Fig. 2), we used a simple inverse modeling approach to calculate the weighted $\delta^{18}O$ composition of rainfall that explains the observed drip water $\delta^{18}O$ baseline values and variability in each chamber (See Supplementary Fig. B). The weighted $\delta^{18}O$ composition of rainfall is based on the sum of all the rainfall events starting from that closest or coeval to the time integrated by each drip water sample collected, and moving back in time integrating previous rainfall events, until the observed drip water $\delta^{18}O$ variability can be explained. The rationale for this approach is that drip water can reflect only rainfall events that are coeval (fast permeability) and/or preceding the time of collection, depending on the reservoir size. The larger the reservoir size, the larger the expected integration time of rainfall amount by drip water samples. Note that in reality the reservoir does not reflect the time domain *per se*, but an amount of rainfall that accumulated over a given amount of time, which is known to vary from intraseasonal to interannual timescales. Ideally, this analysis would be based on characterizing the precipitation amount and isotopic composition of every single rainfall event. Practically, that was not possible for us, and rainfall $\delta^{18}O$ samples integrate precipitation between 1–59 days. Our protocol, however, was sufficient to closely approximate the integration time of drips from the three chambers examined at Río Secreto Cave (Section 4.4; Fig. 2).

3.3.3. Convergence of drip water $\delta^{18}O$ values

If different drip sites integrate rainfall amount accumulated over different periods of time, depending on the size of their reservoirs, their drip water $\delta^{18}O$ values are expected to be different at a given point in time. Nevertheless, the amount-weighted $\delta^{18}O$ composition of drip water at different locations integrated over a sufficiently long period should converge into a single value, provided that no other effect, such as evaporation, has altered the isotopic composition of the water source. In order to test this notion, we calculated the amount-weighted $\delta^{18}O$ composition of each drip, integrating consecutively from 2 to 22 months of water accumulation, in order to find the integration time of convergence. We note that this study allows us to perform this integration because all the drip water that drained over two years was collected for each of seven drip sites (see Supplementary Tables A and B). We also calculate amount-weighted and unweighted $\delta^{18}O$ compositions of each drip site to compare each other (Table 1).

4. RESULTS

This study presents results for the hydrological years spanning June 2017-May 2018 and June 2018-April 2019, which represent the fourth and fifth year (hereafter referred to as Y4 and Y5) of a continuous monitoring effort that was initiated during the hydrological year June-2014–May 2015

Table 1
Statistical summary of rainfall, drip water and groundwater $\delta^{18}O$ and δD collected at Río Secreto Cave during July 2017–April 2019. All isotopic values are reported in ‰ relative to V-SMOW.

Sample	n	$\delta^{18}O$ AVG	$\delta^{18}O$ 1 SD	$\delta^{18}O$ MIN	$\delta^{18}O$ MAX	δD AVG	δD 1 SD	δD MIN	δD MAX	$\delta^{18}O$ Amount - Weighted AVG	δD Amount - Weighted AVG	number of available volume data
Monthly Rainfall	22	−3.2	1.6	−6.9	−0.6	−12.8	14.5	−46.6	6.8	−3.3	−15.3	22
B4	16	−3.8	0.5	−4.5	−3.2	−18.5	2.3	−21.9	−14.4	−3.9	−19.5	13
B1	20	−3.6	0.6	−4.4	−2.8	−16.6	5.1	−27.1	−9.0	−3.9	−19.5	18
Atila	16	−4.0	0.3	−4.4	−3.3	−20.6	0.9	−22.1	−18.9	−4.0	−20.5	15
A7	14	−3.7	0.7	−4.5	−2.2	−18.9	5.2	−24.0	−7.7	−3.8	−20.0	11
A3	14	−3.9	0.3	−4.4	−3.2	−19.1	2.0	−22.1	−15.3	−4.0	−19.4	11
LF1	20	−2.5	0.7	−3.6	−1.4	−9.0	5.2	−16.2	−1.4	−2.5	−9.2	16
Fénix	20	−4.8	0.4	−5.6	−4.0	−27.4	2.8	−30.5	−22.6	−4.9	−27.5	18
LF Station Pond	12	−3.5	0.7	−4.4	−2.3	−18.1	3.4	−23.3	−13.1			
A Station Groundwater	13	−4.6	0.3	−5.0	−4.2	−26.7	1.0	−29.1	−25.2			

(LH19). We place our results in the context of evidence from the previous three hydrological years (hereafter referred to as Y1, Y2 and Y3) which established the long-term relationship between precipitation amount and its isotopic composition, and in turn how Y4 and Y5 results relate to temporal variability in the isotopic composition of drip water. Also, this study centers preferentially on $\delta^{18}O$ (and not δD), because of its application as a proxy of precipitation in stalagmite records from tropical and subtropical regions.

4.1. Precipitation amount, $\delta^{18}O$ and δD composition

The records of rainfall amount from Río Secreto and the government meteorological station in Playa del Carmen (i.e. CONAGUA) were similar to each other during the five hydrological years of monitoring (Supplementary Table A). Precipitation amount during the hydrological year Y4 was particularly large (1513 mm/yr) relative to the previous year when the YP experienced a summer drought (748 mm/yr) and slightly greater than the long-term annual average (1998–2011 = ~1400 mm/yr; Supplementary Table E). Precipitation amount during Y5 was also significantly lower than the average and represents another drought year (798 mm/yr). A drought year in this study, therefore, is understood as a hydrological year when annual rainfall amount represented 53–57% (Y3 and Y5, respectively) of the instrumental 14-year annual average rainfall amount (1998–2011; Supplementary Table E).

The $\delta^{18}O$ and δD annual amount-weighted isotopic compositions of rainfall were, respectively −4.1‰ and −22.5‰ during Y4, and −2.9‰ and −9.5‰, during Y5. The $\delta^{18}O$ composition of rainfall during Y4 is therefore significantly more negative than the previous year Y3 (-2.3 ‰) and proceeding year Y5 (-2.9‰), when the YP experienced significant summer droughts and positive rainfall $\delta^{18}O$ anomalies. During both years, rainfall $\delta^{18}O$ and δD varied from −6.9‰ to −0.6‰ and from −46.6‰ to +6‰, respectively (n = 35) (Fig. 2); this is almost the same intra-annual $\delta^{18}O$ amplitude variability reported for the three previous hydrological years by LH19 (~6.8‰ for $\delta^{18}O$). Monthly rainfall $\delta^{18}O$ values show two distinctive negative excursions reaching peak values of ~−7 ‰ occurring in July/August 2017 and May/June 2018 relative to the preceding samples, reflecting the low rainfall isotopic signal of tropical cyclones Franklin and Alberto. Lower rainfall isotopic values are observed in association with the rainy seasons (June-Sept) and relatively more positive with the dry seasons (March-May), consistent with observations of previous years and the amount effect relationship characterized on seasonal timescales by LH19.

We found a negative relationship between the annual amount-weighted $\delta^{18}O$ composition of rainfall and annual rainfall amount during the 5 hydrological years (slope of −0.0019 ‰ per mm, $r^2 = 0.37$), revealing the existence of an interannual amount effect. If we remove from this linear regression the data from Y4 -which represents an anomalously wet year-, we found a significantly stronger interannual amount effect (slope of −0.0066 ‰ per mm, $r^2 = 0.82$; Fig. 3A). The amount effect slope value from this study is

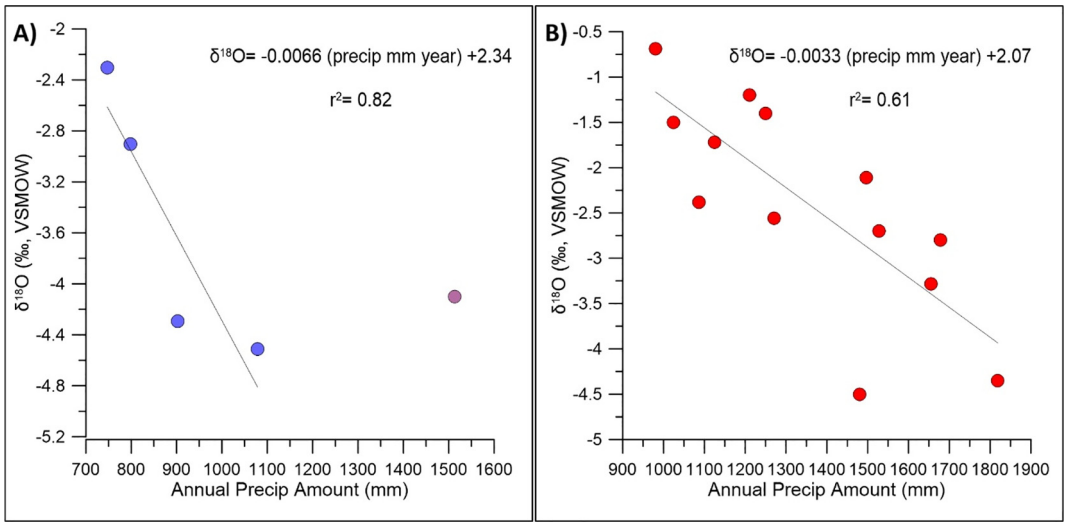

Fig. 3. (A) Rio Secreto annual rainfall amount and $\delta^{18}O$ composition during 5 hydrological years (See Sections 4.1 and 5.1). Note that the outlier point is not considering for the linear regression. Data of three hydrological years is from Lases-Hernandez et al. (2019). (B) Havana, Cuba annual rainfall amount and $\delta^{18}O$ composition during 12 hydrological years (IAEA-GNIP, 2002–2015). Linear regressions between annual precipitation amount and $\delta^{18}O$ composition from each location are shown.

very similar to that observed in Cuba (Fig. 3B) and to those suggested by climate models with isotope tracers (Vuille et al., 2003)

4.2. Drip $\delta^{18}O$ variability

All drip water isotopic data are reported in Supplementary Table B and a statistical summary is presented in Table 1. A total of 127 samples from 7 different drip sites were analyzed for $\delta^{18}O$ and δD. These samples represent uninterrupted periods of drip water accumulation from 3 to 61 days over the time interval from July 2017 to April 2019. In addition we collected a total of 5 discrete samples during two visits to the cave from hollow inverted-funnel-shaped stalactitic speleothems that discharged a large volume of water after few hours of the occurrence of strong rainfall events (also called showerhead). Drip water $\delta^{18}O$ and δD varied from $-5.6‰$ to $-1.4‰$ and from $-30.5‰$ to $-1.4‰$, respectively. The lowest isotopic values correspond to Fénix drip site and the most positive to LF1 drip site (Fig. 2).

4.2.1. Local meteoric Water Line and Drip Water Line

The Global meteoric Water Line is the established linear correlation between $\delta^{18}O$ and δD of meteoric precipitation that follows the relationship $\delta D = 8\ \delta^{18}O + 10‰$ at a global scale (Craig, 1961; Rozanski et al. 1993). At a regional level it can vary because local effects can influence the isotopic composition of rainfall and therefore a Local Meteoric Water Line (LMWL) should be established by data spanning at least one hydrological cycle (Clark and Fritz, 1997). LH19 characterized the LMWL finding a slope of 8.2 for rainfall within the period Y1-Y3. The LMWL for the period Y4-Y5 has a slope of 8.8, slightly higher than that found for the previous period (Table C in Supplementary material). However, a comparison between the $\delta^{18}O$ and δD values of drip water from this study with the coeval LMWL, shows that practically none of the drip water values deviate markedly from the LMWL. Moreover, drip water $\delta^{18}O$ and δD values plot very close to those of rainfall samples that represented rainfall amounts higher than 90 mm, which together represent 80% of total rainfall amount during the period Y4-Y5 (Fig. C Supplementary material).

4.3. Drip water $\delta^{18}O$ amplitude

We examine the drip $\delta^{18}O$ amplitude observed in this study based on cumulative drip water samples in light of the previous monitoring work by LH19 based on the collection of discrete water samples. At Station A station, the $\delta^{18}O$ amplitude variability of drip sites A3, A7 and Atila was 1.6‰, 1.6‰ and 1.2‰, respectively (Y1-Y3), and 1.2‰, 2.8‰ and 1.2‰, respectively, during this study period. At Station B, the $\delta^{18}O$ amplitude variability range (2 SD) of drip sites B1 and B4 was 3.2‰ and 2.4‰, respectively (Y1-Y3), and 2.4 ‰ and 2‰, respectively during this study period (Y4-Y5). At Station LF, LF1 and Fénix showed an amplitude range of 4‰ and 0.8‰ (2 SD respectively) during the three years preceding this study and a range of 2.8‰ and 1.6‰, respectively, during this study period.

As determined in LH19, drips from the three different chambers reflect the $\delta^{18}O$ amplitude variability of rainfall to different extents. Across the five years of monitoring in Río Secreto cave the largest drip water $\delta^{18}O$ value range is observed at LF1 site (5‰), followed by drip sites from Station B (4‰) and lastly drip sites from Station A (2‰). Fénix is an exception in that it records the lowest amplitude variability of all drip sites (~1‰) and its $\delta^{18}O$ values are consistently more negative than those of average rainfall. The observed drip water $\delta^{18}O$ amplitude variability ($\leq$4 ‰) for Y4 and Y5 is smaller than that of rainfall

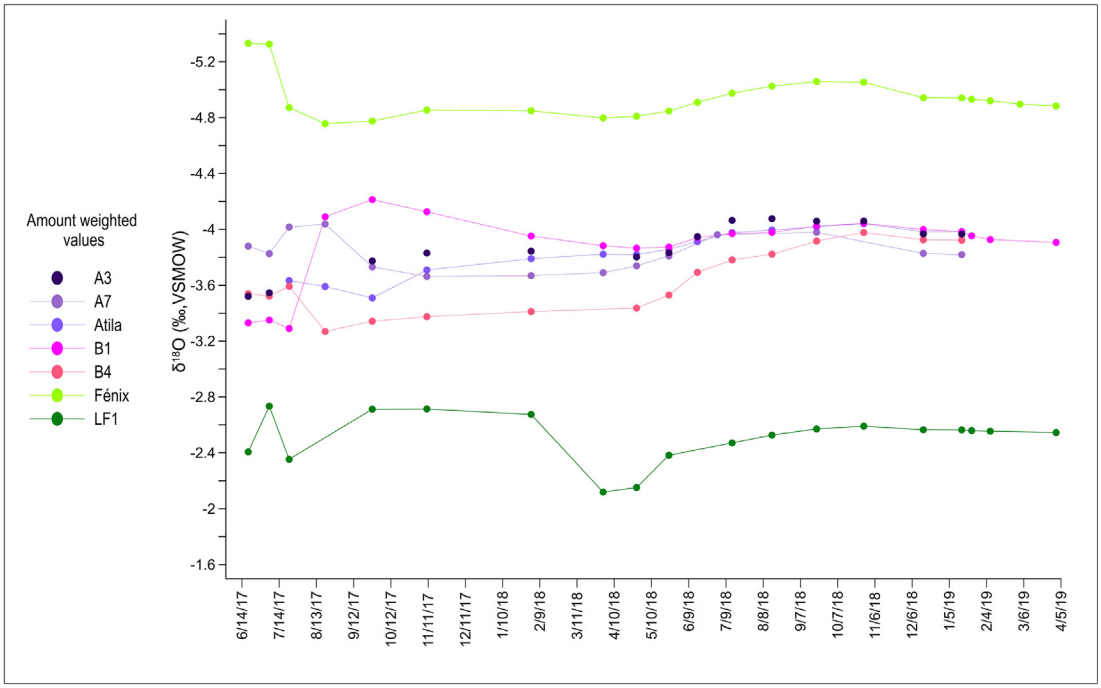

Fig. 4. Río Secreto amount weighted $\delta^{18}O$ composition of drip water for this study (Y4 and Y5). The first values (6/14/17) represent the $\delta^{18}O$ composition of drip water during the first month, the second values represent the amount weighted $\delta^{18}O$ composition integrating the first and the water sample collected subsequently (7/14/17), the third values represent the amount weighted $\delta^{18}O$ composition integrating the first three samples, and so on (See Sections 3.3.3 and 4.4). As described in the main text, each sample represents the total water accumulated over a specific time interval which may differ among drip sites and can be from about a month or longer.

(6‰) for this period, as was previously reported for Y1-Y3 by LH19.

4.4. Drip water isotopic integration of rainfall and convergence

As noted above, monitored drips from all three chambers integrate a longer time interval than monthly $\delta^{18}O$ rainfall variability (~6‰, 2SD). As described in the methods Section 3.3.3, we can determine the integration time of rainfall amount necessary to explain the observed drip water $\delta^{18}O$ composition. Fig. 2 shows the different time integrations of rainfall amount that can explain most of the variability in drip water $\delta^{18}O$ observed in Stations LF, A and B. As expected from the observed difference in the $\delta^{18}O$ amplitude variability of drip water among the three different chambers, the shortest integration time corresponds to LF1 (2–3 months) and the longest to drip sites at Station A (15 months). Drip water at Station B represents rainfall integration times between these two end members (4 months). Note that our approach explains not only the observed drip water $\delta^{18}O$ variability, but also closely approximates the absolute values, with some exceptions. LF1 $\delta^{18}O$ values tend to be more positive than those of rainfall during Y1, Y2 and Y4 and drip sites from Stations B and A tend to be more negative during the drought years Y3 and Y5 (Fig. 2).

Because the various drip locations represent different integration times of rainfall, their observed $\delta^{18}O$ composition is not the same at a given point in time, even when they ultimately reflect the isotopic composition of the same rainfall source. Provided drip water is integrated over a sufficiently long interval, however, the $\delta^{18}O$ composition from all drip sites should converge into a single value reflecting the isotopic composition of the source; if it remained unaltered by evaporation or some other process. In order to find the integration time of convergence we calculated the amount-weighted $\delta^{18}O$ composition of each drip, integrating consecutively from 2 to 22 months of water accumulation (Fig. 4). The results of this analysis indicate that drip water from Stations A and B converge into a single $\delta^{18}O$ value after an integration time of about 11–15 months, and that LF1 and Fénix are isotopically distinctive. Of all the drip sites, LF1 integrated $\delta^{18}O$ values are the most positive and those from Fénix the most negative, consistently (Fig. 4).

In Table 2 we present a summary of the isotopic and discharge characteristics of the 7 drips analyzed in this study, based on the data from 5 hydrological years. We found that the drip sites that have higher $\delta^{18}O$ variability and closer to that of rainfall are those that have a shorter rainfall accumulation time and therefore probably have smaller reservoirs (e.g. LF1, B1 and B4). However, short rainfall integration times and greater variability may be associated with discharges classified as seepage flow (e.g. B4 site) and also seasonal drips (e.g. LF1, B1)(Table 2). The opposite can also occur; long rainfall integration times can correspond to both, seasonal drips (e.g. Atila) and a seepage flow (e.g. A3 and A7).

Table 2
Summary of isotopic and discharge characteristics of 7 drip sites based on 5 year data for the period June 2014–April 2019 from Río Secreto cave. All results and inferences are explained in detail in Sections 4 and 5. To perform calculations, data before July 2017 was obtained from Lases-Hernandez et al. (2019). All isotopic values are reported in ‰ relative to V-SMOW.

Sample	$\delta^{18}O$ AVG	$\delta^{18}O$ 1SD	$\delta^{18}O$ range	% of $\delta^{18}O$ rainfall range	$\delta^{18}O$ (n)	drip rate avg (mL/h)	drip rate 1 SD (mL/h)	drip rate max (mL/h)	drip rate range (mL/h)	drip rate (n)	Classification	Rainfall integration time (months)	Isotopic convergence time (months)
A3	−4.2	0.4	2.1	31	116	2.4	1.7	10.8	10.5	115	Seepage flow	15	11
B4	−4.0	0.6	2.8	41	79	3.0	1.9	9.7	9.1	74	Seepage flow	4	15
A7	−4.2	0.5	2.6	38	69	3.3	1.4	8.3	8	67	Seepage flow	15	11
Atila	−4.3	0.4	1.8	26	63	3.2	1.9	11.8	11.5	55	Seasonal drip	15	11
Fénix	−5.4	0.4	1.8	26	86	3.9	1.9	15.3	14.8	87	Seasonal drip		
LF1	−2.4	1.0	4.9	72	102	1.2	1.2	9.2	9.1	99	Seasonal drip	1 to 3	
B1	−3.6	0.7	4.9	72	135	3.4	4.3	25.1	25	117	Seasonal drip	4	11

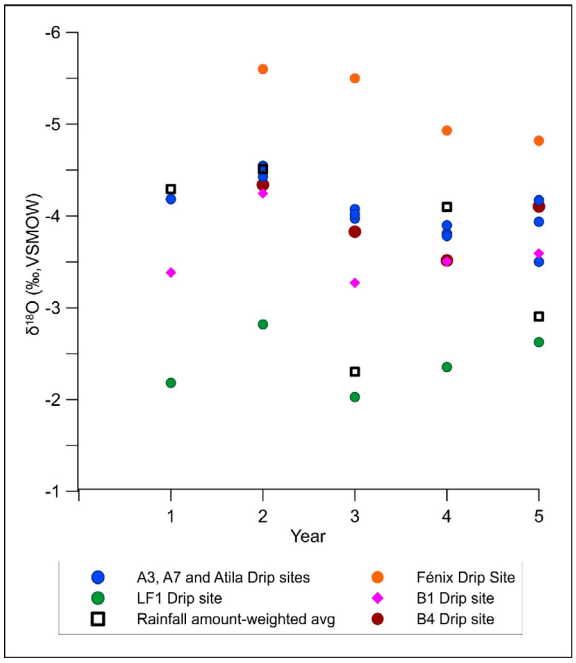

Fig. 5. Río Secreto annual amount-weighted $\delta^{18}O$ composition of rainfall and drip water at stations A, B and LF. Values were calculated from June 2014 to May 2015 (year 1), June 2015 to May 2016 (year 2), June 2016 to May 2017 (year 3), June 2017 to May 2018 (year 4) and June 2018 to April 2019 (year 5). Values of A3, A7, Atila and B4 drip sites at year 5 only integrate the $\delta^{18}O$ averages of 8 months (See Section 4.6). Data of the three first hydrological years are from Lases-Hernandez et al. (2019).

4.5. Annual drip water $\delta^{18}O$

The new monitoring effort consisting of cumulative samples allow us to determine an annual amount-weighted $\delta^{18}O$ composition of each drip site and place the information from previous years in the context of the last five years of rainfall information.

Because of the discrete sampling protocol followed by LH19, it was not clear whether drips LF1 and LF2 (not investigated here), which had the most positive annual $\delta^{18}O$ compositions of all 16 drip sites, reflected evaporation processes or that the discrete sampling protocol did not allow accurate characterization of their annual amount-weighted $\delta^{18}O$ composition. We note that drips LF1 and LF2 showed the largest $\delta^{18}O$ amplitude variability of all drip sites and the closest to that of rainfall. Therefore, as mention before, averaging the isotopic composition of discrete drip water samples would be equivalent to calculating the average annual $\delta^{18}O$ composition of rainfall without weighing sample amount. In fact, the annual $\delta^{18}O$ composition of these drips closely resembled the annual amount-unweighted $\delta^{18}O$ composition of rainfall during Y1-Y3 (LH19).

We find that during Y4 and Y5 the annual amount-weighted and unweighted $\delta^{18}O$ composition of drip water was the same to within 0.1‰ in six of the seven drip sites examined (Table 1). LF1 is persistently more positive (~1–2‰) than the amount-weighted and unweighted $\delta^{18}O$

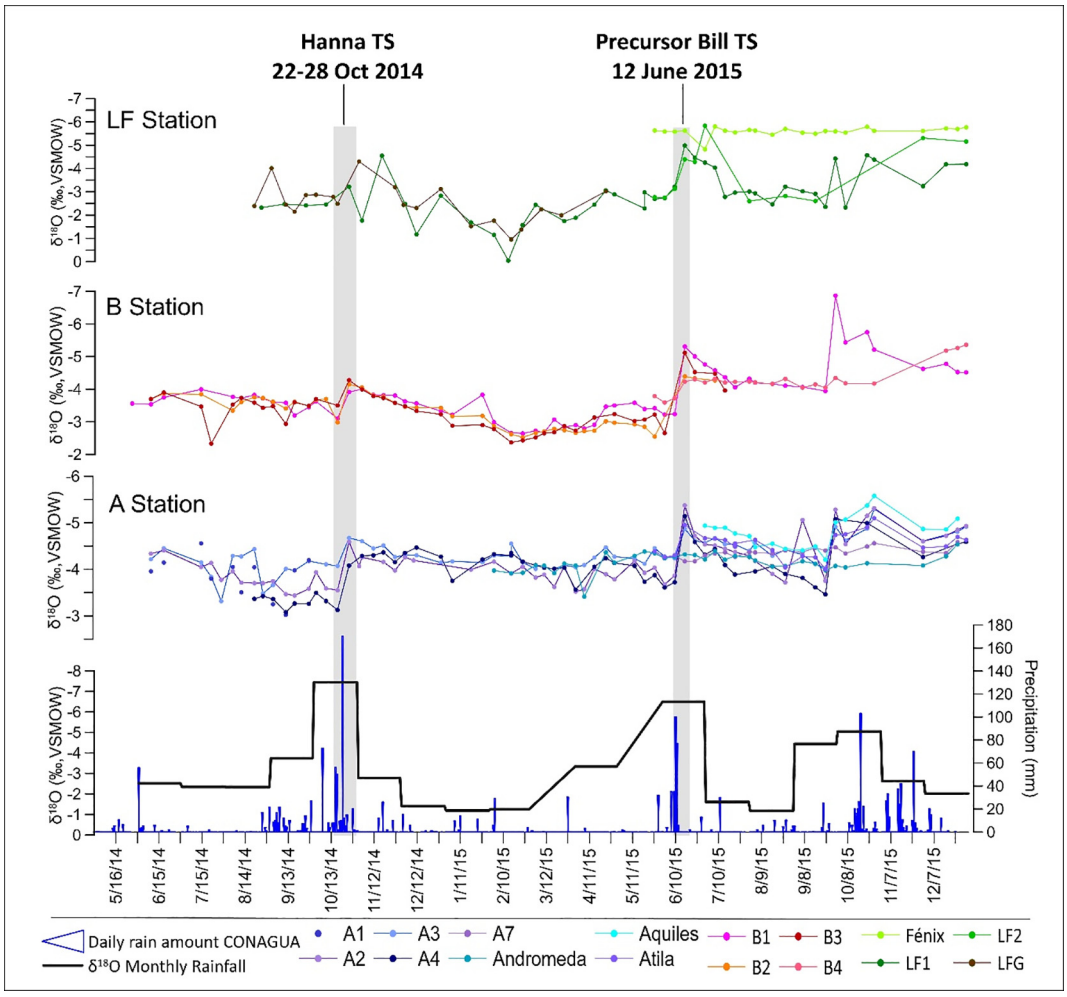

Fig. 6. Upper three panels: drip water $\delta^{18}O$ time series from June 2014 to December 2015 (Y1 and Y2) from stations LF, B and A. Lower panel: monthly rainfall $\delta^{18}O$ values (black line) and amount of daily precipitation from CONAGUA government station (Fig. 1A). Note that the Y axis values are inverted. Gray bars highlight the time interval when tropical cyclones influenced the site. Data was obtained from Lases-Hernandez et al. (2019).

composition of rainfall and all other drip sites from Stations A and B (Table 1). This result concerning LF1 is similar to what was observed during the previous three years (Y1-Y3) suggesting that this drip site reflects precipitation variability but also is influenced by evaporation at the surface as it is discussed in Section 5.4, below.

4.6. Interannual variability of drip water and rainfall $\delta^{18}O$

Fig. 5 shows a comparison of the annual amount-weighted $\delta^{18}O$ composition of rainfall during Y1-Y5 relative to the annual $\delta^{18}O$ composition of drip water during Y1-Y3 (amount-unweighted) and years Y4-Y5 (amount-weighted). As pointed out above, with the exception of LF1, the amount-unweighted and weighted $\delta^{18}O$ composition of drip water were almost the same during Y4 and Y5. Therefore, despite the previous sampling protocol being discrete, it is possible that the annual $\delta^{18}O$ composition of drips during Y1-Y3 also approximates their amount-weighted $\delta^{18}O$ composition, probably because of the high sampling frequency (bi-weekly) in combination with the reservoir integration.

During Y1, Y2 and Y4, the annual isotopic composition at drips sites from Stations A and B are similar to the annual $\delta^{18}O$ composition of rainfall (Fig. 5). During the drought years Y3 and Y5, however, when the annual isotopic composition of rainfall shifts to become 1–2 ‰ more positive than their corresponding preceding years, the isotopic composition at these drip sites are typically more negative than those of rainfall. More specifically, During Y3, the isotopic composition of rainfall shifted by +2 ‰ relative to Y2 whereas drips from A and B Stations only shifted by +0.5 ‰ and ~+1‰, respectively (Fig. 5) (LH19). During Y5 the isotopic composition of rainfall shifted by +1‰ relative to Y4. Drips from Station A remained practically unchanged or shifted negatively only slightly by ~−0.2‰ from Y4 to Y5. Drip B4, in contrast shifted negatively by ~−0.7‰, as if still catching up with the wet

negative isotopic year Y4, whereas drip B1, remained unchanged from Y4 to Y5. Exceptions to these patterns are drip sites LF1 and Fénix. LF1 annual $\delta^{18}O$ values vary in the same direction as annual shifts in rainfall $\delta^{18}O$ (except in Y5) but they are consistently more positive than rainfall and the other drip sites (Fig. 5). Annual isotopic composition of Fénix shows a progressive interannual positive shift from Y2 to Y5 and its absolute $\delta^{18}O$ values are consistently 1-3‰ more negative than those of rainfall amount-weighted composition for Y2-Y5 (Fig. 5).

4.7. Discharge

All the primary data of drip water discharge rate and volume changes over time are reported in Supplementary Table B. An important aspect of this study is that it characterizes the total volume of drip water that drained over the full two-year period examined (i.e. Y4 and Y5). During this sampling interval we observe discharge rates that are more variable that those reported by LH19 following a discrete sample collection protocol. The reason for this difference is that this more comprehensive study allows proper characterization of maximum discharge rates. LH19 used graduated cylinders to collect drip water over a 48 hour period, and when water drained during intervals of maximum discharge the containers may have been overfilled (Section 3.3 in LH19). Maximum discharge rates characterized by the protocol by LH19 was 8 mL/hour, whereas this study shows maximum discharge rates of up to 25 mL/hr. We note, however, that only 17 out of 112 samples collected had discharge rates equal or higher than 8 mL/hr. suggesting that LH19's protocol represents a good approximation of typical drip rates while under-representing rare more extreme infiltration events. However, we want also to point out that during Y4 the rainfall amount was higher than during the 3 previous years, therefore the high drip rates characterized at this study may be related to the sampling methodology but also to the increase of recharge into the epikarst during year 4. In this study, we reexamine the hydrological behavior of 7 drips according to the classification of Fairchild et al. (2006), determined by LH19 by examining the first three hydrological years (Fig. 7 at

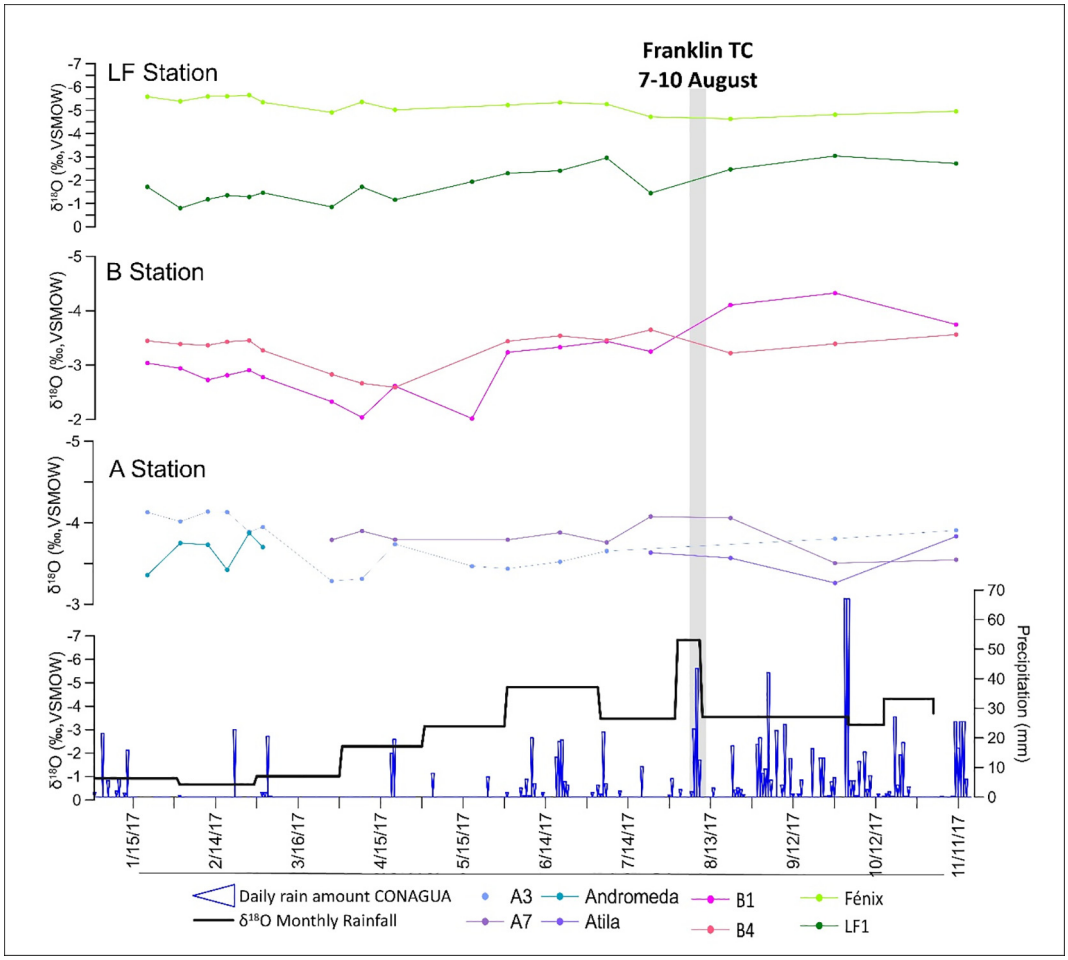

Fig. 7. Upper three panels: drip water $\delta^{18}O$ time series from January 2017 to December 2017 from stations LF, B and A. Lower panel: monthly rainfall $\delta^{18}O$ values (black line) and daily rainfall amount from CONAGUA weather station (Fig. 1A). Y axis values are inverted. Gray bar highlight the time interval when Franklin tropical cyclone influenced the site. Data previous to July 2017 was obtained from Lases-Hernandez et al. (2019).

LH19). We confirm their classification for six out of the seven drips sites studied during years 4 and 5, the exception being Fénix, previously classified as Seepage Flow (Fig. 7 at LH19) and now reclassified as a Seasonal drip (Supplementary Fig. A). Lastly, we find that there is no significant linear relationship (95% confidence interval) between drip water $\delta^{18}O$ and discharge rates, at all 7 drip sites monitored during Y4 and Y5, with the exception of A3 ($r^2 = 0.35$, $p = 0.043$).

4.8. Groundwater $\delta^{18}O$ variability

A total of 25 samples of groundwater from standing water at Stations LF (12 samples) and A (13 samples) were collected from August 2017 to January 2019 and analyzed for $\delta^{18}O$ and δD (Supplementary Table C). In comparison to monitored drips located in the LF chamber, the $\delta^{18}O$ composition of groundwater from Station LF is more negative than that of drip water from LF1 and more positive than Fénix. LF groundwater is also isotopically more positive than drip water at all other drip sites from Stations A and B, and groundwater from Station A (by up to 1.5‰). The underground pool at Station A is deeper and clearly connected with the rest of the groundwater system. We have observed that during periods of water table rising in the Río Secreto Cave system, groundwater in LF rises as well, but in contrast with Station A, LF is close to a collapsed sinkhole and thus exposed to ventilation. Therefore, it was not surprising to find that the water table in LF chamber is highly variable and likely experiences evaporation. However, when plotting $\delta^{18}O$ and δD values of LF groundwater, most of them do not deviate markedly form the LMWL calculated for this study (Fig. C Supplementary material).

4.9. $\delta^{18}O$ composition of tropical cyclones

This study characterizes the isotopic signature of two weak tropical cyclones (TCs) that influenced the YP: Franklin (1–9 August 2017), which had a $\delta^{18}O$ value of −6.8‰ and a local rainfall flux of 89 mm, and Alberto (25–26 May, 2018) with a $\delta^{18}O$ of −6.9‰ and 102 mm of rainfall. Franklin made landfall over the YP with tropical storm intensity and weakened until re-emerging in the Gulf

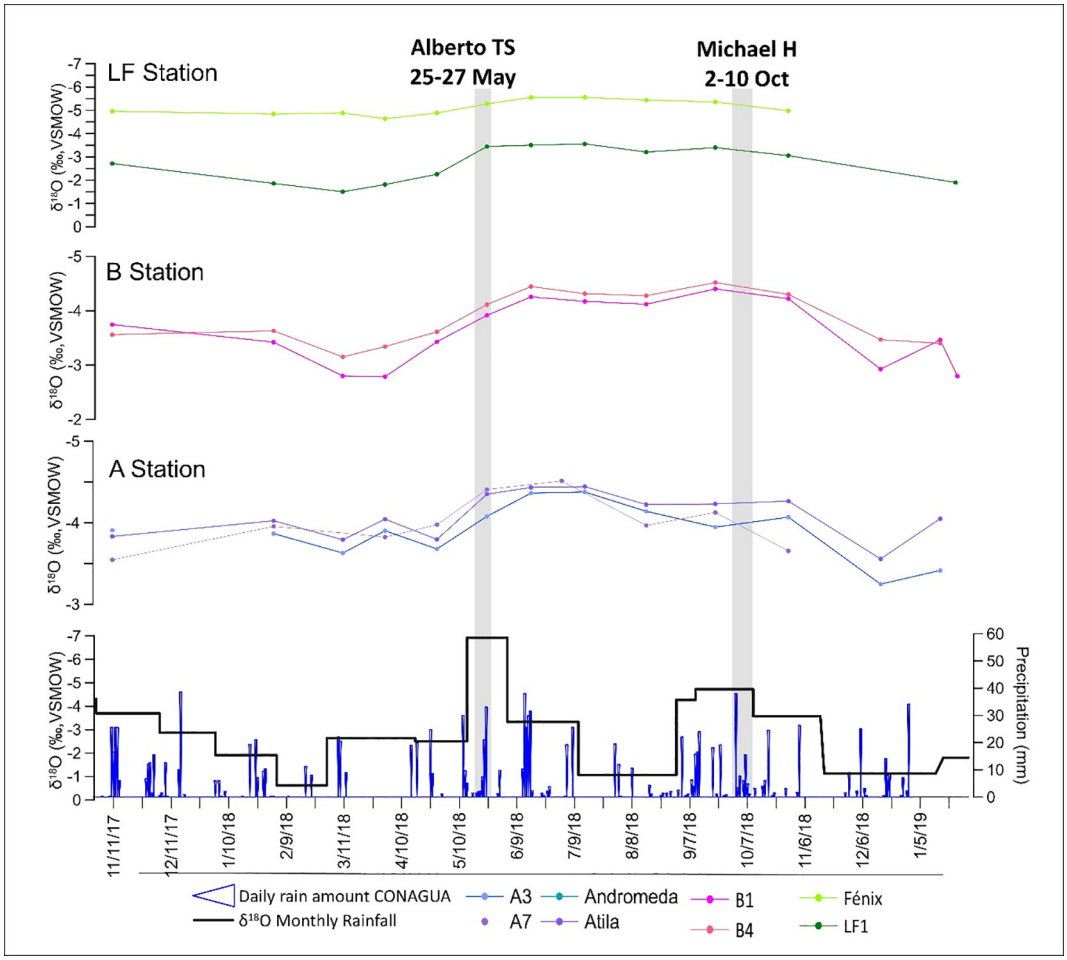

Fig. 8. Upper three panels: drip water $\delta^{18}O$ time series from November 2017 to April 2019 from stations LF, B and A. Lower panel: monthly rainfall $\delta^{18}O$ values (black line) and daily rainfall amount from CONAGUA weather station (Fig. 1A). Y axis values are inverted. Gray bars highlight the time interval when tropical cyclones influenced the site.

of Campeche to become a hurricane, while Alberto skirted the YP coast as it developed into a subtropical depression before intensifying to a tropical storm over the Gulf of Mexico. These two locally-weak TC events produced precipitation with the lowest isotopic values found in this study: a negative isotopic shift of ~4 ‰ relative to the isotopic composition of rainfall accumulated over the month prior to the events. In addition, rainfall associated with these TCs had $\delta^{18}O$ compositions distinctively more depleted (2–4‰) than rainfall events that were not associated with TCs, of similar or even higher amount fluxes. TC Michael (5–8 October, 2018), whose rainfall was very strong in other regions (e.g. Florida), did not produce significant rainfall in the study area.

4.10. Response of $\delta^{18}O$ dripwater to tropical cyclones

The influence of TCs Franklin and Alberto on the isotopic composition of drip water can be observed at some drip sites even when the sample protocol implemented in this study involved ~ monthly water accumulations (Figs. 7 and 8). Specifically, the negative rainfall $\delta^{18}O$ composition associated with Franklin is reflected as a negative $\delta^{18}O$ departure from background levels of −1‰ and −0.9‰ in LF1 and B1 drip sites, respectively (Supplementary Table D). This event, however, is not observed at the other five drip sites because of the lower-resolution sampling protocol. While rainfall was collected from August 1–9, 2017, exactly when Franklin affected the locale, drip water was collected over a full month (from August 2 to September 8, 2017).

Regarding TC Alberto, rainwater and drip water were collected during the same period of time (14 May-4 June 2018). With this higher drip water collection frequency, the distinctively low $\delta^{18}O$ signature associated with Alberto was registered within weeks as a negative shift of −1.2 ‰ by LF1, and of ~−0.5 ‰ by the other 6 drip sites (Fig. 8; Supplementary Table D). Therefore, Franklin's distinctive rainfall negative isotopic signal was likely dampened by other rainfall events occurring over that period.

We point out that during the previous weekly to biweekly sampling protocol of drip water performed by LH19, the isotopic response of drip sites to TC rainfall was recorded by drip sites from all chambers, with the exception of Fénix. An example is the negative rainfall isotopic shift associated with TC Hanna (October 21, 2014), which is the most negative rainfall water sample (−9.5‰) recorded in Río Secreto during the five hydrological years (Supplementary Table A). Because Hanna´s rainfall amount was only 79 mm whereas the total amount of rainfall in October 2014 was 325 mm, the isotopic shift if comparing September 2014 monthly rainfall to Hanna´s rainfall was of −5.8‰, while the isotopic shift from September to October 2014 monthly rainfall was only −3.7‰, making it clear that it is necessary to monitor at least at weekly basis in order to capture the full shift associated with TC´s rainfall in both rainfall and drip water samples (Supplementary Tables A and D). During September-October 2014 Río Secreto drip water monitoring included only 6 drip sites, three of them examined also in the present study, and all of these presented a negative shift of up to −1.8‰ associated with Hanna TC rainfall (Fig. 6 and Supplementary Table D). As another example, high-resolution sampling of drip water from nine drip sites, including five of the seven examined in the present study, allowed detection of the low $\delta^{18}O$ shift associated with TC Bill rainfall (June 9–16, 2015). Drip water $\delta^{18}O$ at these nine drip sites shifted by up to −2.1‰ relative to the background (Supplementary Table D). This response was particularly noteworthy because the sample containing rainfall from TC Bill represented the accumulation of one month of rainfall (June) and its isotopic composition was 3.2‰ more negative than the sample of the previous month (April). In this case, however, the high-resolution cave sampling protocol allowed the detection of the isotopic signature of this TC in drip water. Because the rainfall sample of TC Bill itself was not measured, the shift in rainfall $\delta^{18}O$ of monthly samples underestimates the shorter term influence of this cyclone on drip water $\delta^{18}O$ (Supplementary Table D).

5. DISCUSSION AND IMPLICATIONS FOR PALEOCLIMATE STUDIES

5.1. *Amount effect* on interannual and seasonal timescales

The isotopic amount effect, whereby higher precipitation amount is associated with lower rainfall isotopic ratios is recognized to exist in tropical and subtropical regions from seasonal to interannual timescales (Dansgaard, 1964; Rozanski et al., 1993; Araguas-Araguas et al., 2000; Vuille et al., 2003). Studies with instrumental records of precipitation that report an amount effect on interannual timescales are scant, however, even though it is a desirable precondition to reconstruct precipitation amount variability from stalagmite $\delta^{18}O$ records. To our knowledge, in addition to evidence from models (i.e. Vuille et al., 2003), studies demonstrating an amount effect on interannual timescales based on instrumental records are scarce. Bar-Matthews and Ayalon (2004) characterized the amount effect on interannual timescales in the eastern Mediterranean region and report a slope of −0.005 ‰ mm^{-1} (similar to this study). Maher and Thompson (2012) also report interannual covariance between rainfall amount and $\delta^{18}O$ values on various Chinese and Indian locations based on IAEA-GNIP data spanning the interval between 1961 and 2003.

Atmospheric general circulation models (i.e. ECHAM-4 and GISS II) used to analyze interannual variability of $\delta^{18}O$ in precipitation in the tropical Americas suggest a significant amount effect on interannual timescales for the YP and Caribbean (Vuille et al., 2003). These models detect an amount effect on interannual timescales in simulations spanning between 16 and 44 years (1979–1994) which is somewhat validated by model comparisons with decadal or longer IAEA instrumental isotope records (Vuille et al., 2003). The nearest IAEA station to Playa del Carmen is the one from Havana, Cuba. Examination of the relationship between annual precipitation amount and $\delta^{18}O$ from Havana indicates an amount effect on interannual timescales ($n = 12$ years, $r^2 = 0.84$, Fig. 3). The present study

presents the first instrumental evidence in support of an amount effect on interannual timescales for the YP. As mentioned in Section 4.1 the correlation between annual rainfall amount and the amount weighted isotopic composition of 4 of 5 years was strong (i.e. Y1,Y2,Y3 and Y5). However, Y4 exhibited higher $\delta^{18}O$ values than expected from the linear correlation of those four years (Fig. 3; Section 4.1). The relatively high annual $\delta^{18}O$ composition during Y4 can be related to mesoscale convective complexes with disorganized convection (Kurita, 2013) as well as the origin and transport of the low-level vapor feeding the convective system that may affect the amount effect (Risi et al. 2008; Rao et al. 2008). In order to improve our understanding of the driving factors of the amount effect on interannual time scales in this region a detailed continuous monitoring effort would be required. We aim at continuing this monitoring effort to help better describe the amount effect on interannual timescales in the region.

During Y4 and Y5, the protocol of this study precludes determining the amount effect on seasonal timescales because of the variable sample time integrations from 3 to 59 days of rainfall. The existence of an amount effect on seasonal timescales in this region, however, has been observed by previous studies (Medina-Elizalde et al., 2016a; Lases-Hernandez et al., 2019).

5.2. Reservoir integration times are relatively fast in Río Secreto cave

In this study we find that most drips retain most of the isotopic amplitude variability observed during the previous discrete sampling protocol (48 hr. water accumulation every 1–2 weeks) (Lases-Hernandez et al., 2019). The reservoirs associated with six of seven drip sites examined integrate between 3 and 15 months of rainfall accumulation. Of course, time is not *per se* the determining factor, but instead the amount of rainfall over time. The observed integration times imply that: (i) drips record preferentially monthly and longer rainfall $\delta^{18}O$ variability; (ii) water discharged at a drip site over few weeks does not represent coeval precipitation, but a combination of coeval and prior precipitation; (iii) even when drip water samples represent short-term isotopic amount-unweighted sample aliquots (e.g. 48 hr.), they can still approximate an annual amount-weighted $\delta^{18}O$ composition at each drip site, as it is observed in this study and; (iv) the longer the integration time and reservoir size, the longer the expected tendency to remain isotopically unchanged (i.e. higher isotopic inertia). We observe that drip sites at Station A and Fénix, with the longest integration times, have the highest isotopic inertia, lagging and underestimating interannual changes in precipitation $\delta^{18}O$ (Fig. 5). Finally, we acknowledge that the estimated integration times do not explain all the drip water $\delta^{18}O$ absolute values because the integration time is not stationary, as previously pointed out by Lases-Hernandez et al., (2019).

When we compare the integration times observed in Río Secreto with those observed in caves elsewhere, we find that the transmission of the isotopic composition of rainfall to drip water is relatively fast. Genty et al. (2014) for example, applied a similar approach to ours (i.e. integration of amount-weighted $\delta^{18}O$ composition of rainfall) and calculated water residence times from 32 to 140 months in drips from shallow galleries in two caves of southern France; Villars and Chauvet caves. Recently, Genty et al. (2014) results were supported by Jean-Baptiste et al. (2019) via a tritium dating of drip water study. In Soreq cave, Israel, it takes between 26 and 36 years for rainwater to reach galleries 10–50 meters below the surface (Kaufman et al., 2003), while it takes only 2–4 years for rainwater to reach 10–30 m deep galleries in Bunker Cave, Germany (Kluge et al., 2010). We note that similar integration times of few months found in this study have also been observed in Borneo where precipitation $\delta^{18}O$ variability is strongly influenced by ENSO (Moerman et al., 2014). Evidently, the comparison of the integration times observed in Río Secreto with those in other caves, highlights the significant potential of this cave for the refining reconstruction of interannual precipitation variability from stalagmite oxygen isotope records and improving proxy uncertainty characterization.

5.3. Implications for stalagmite $\delta^{18}O$ records

The annual $\delta^{18}O$ composition of drip water at Stations A and B was similar to the annual isotopic composition of rainfall during years 1, 2 and 4, but not during the drought years, Y3 and Y5 (Fig. 5). This pattern results from the isotopic inertia associated with the observed rainfall integration times by reservoirs described above. The large isotopic inertia observed in drip sites Fénix and B4 is clearly expressed as a lag of over one year relative to the positive isotopic annual shifts of rainfall (Fig. 5).

The isotopic response of drips from Stations A and B observed during the transition between the wet year Y2 and the drought year Y3 offers a key opportunity to estimate the integration time of one year of drip water accumulation. This is important for high-resolution paleo-rainfall reconstructions from stalagmite $\delta^{18}O$ records. Because of the observed integration times, an annually-resolved stalagmite $\delta^{18}O$ record reflecting the isotopic composition of drips from Stations A and B, would not be expected to reflect only coeval rainfall. Similarly to our approach to assess weekly and monthly drip water isotopic variability, we determined the integration time of rainfall necessary to explain the observed annual isotopic composition of drips from Station A and B1, during Y3. This integration time is 30 months for Station A drip sites and 24 months for drip B1. The implications of these results for paleoclimate reconstructions from stalagmite $\delta^{18}O$ records are significant. These results imply that the annual isotopic composition of drips at Stations A and B1 are similar to that of rainfall during years 1, 2 and 4 simply because the precipitation amount and associated isotopic composition of those years represent the norm, and not because, as is generally assumed implicitly, the drips are exactly integrating a coeval year of rainfall amount.

During consecutive drought years, the volume of an epikarst drip water source reservoir is expected to decline and, as a result, the drip $\delta^{18}O$ composition would rise slowly compared to rainfall $\delta^{18}O$ values (because of the amount effect) and the capacity for pre-drought water to generate

isotopic inertia in dripwater $\delta^{18}O$ values would decline. In this case, a copious rainfall event with an isotopic signature distinctive from that of the reservoir (e.g. from a TC) would be clearly expressed in drip water. In contrast, during consecutive "normal" or wet years, the volume of a reservoir is expected to be relatively large and have a low isotopic signature (the result of the amount effect). The reservoir would have high potential for isotopic inertia and thus remain unaffected by sparse and "normal" rainfall events and mask the negative isotopic signal of TCs.

Stalagmite $\delta^{18}O$ records are therefore expected to register the timing and magnitude of shifts from a drought year to a wet year more accurately than the transition from a wet to a drought year, as observed in this dripwater study. If this is a common regional behavior, stalagmite $\delta^{18}O$ records from the Maya Lowlands may underestimate the magnitude of the droughts associated with the disintegration of the Maya civilization during the Pre-Classic Period (C.E. 100–200) (Medina-Elizalde et al., 2016a) and the Terminal Classic Period (C.E. 750–950) (Medina-Elizalde et al., 2010, Medina-Elizalde and Rohling, 2012, Kennett et al., 2012). Hydroclimate records based on the hydrogen and carbon isotopic composition of leaf wax lipids actually suggest that droughts during the Classic Period were more severe than suggested by other hydroclimate records, including stalagmite $\delta^{18}O$ records (Douglas et al., 2015). The results of this study can help explain this difference.

Due to the central importance of individual drip water reservoirs and routing hydrological characteristics, the timing of the onset and end of drought events as reflected in stalagmite $\delta^{18}O$ records can be expected to differ by months to years. This instrumental study shows that stalagmite sensitivity to TC $\delta^{18}O$ signals is also differentially affected by background hydroclimate, as was inferred by Frappier (2013). Increased isotopic contrast and event rainfall amount relative to epikarst reservoir storage during and following droughts will tend to increase stalagmite $\delta^{18}O$ record sensitivity to TC events. The isotopic effect of TC events during droughts may be difficult to distinguish from drought cessation, unless isotopic shifts are sufficiently anomalous from values expected under normal wet conditions. During wet periods, both brief dry spells and TCs signals in stalagmite $\delta^{18}O$ records are more difficult to distinguish from background, and isotopic inertia from large-volume epikarst reservoirs enhances the tendency to underestimate rainfall variability. The implications of these results should be carefully considered when interpreting stalagmite $\delta^{18}O$ records from locales where the reservoir integration time is large, in those records, slight isotopic variability may be a reflection of much larger shifts in precipitation than suspected. Observing such non-linear effects in this essential paleoclimate proxy system indicates a critical need for further observational and modeling work to re-visit uncertainty analysis and data interpretation for low-latitude $\delta^{18}O$-based paleo-rainfall proxies.

5.4. The LF1 and Fénix anomaly

LF1 represents the drip site with the isotopic amplitude variability closest to that of rainfall, on a weekly and monthly basis. Unfortunately, it fails to capture the absolute rainfall isotopic values. LH19 presented several lines of evidence that surface evaporation and evaporation within Station LF were expected to be minimal: (i) drip water mean annual $\delta^{18}O$ compositions from Stations A and B closely resembled the annual amount-weighted $\delta^{18}O$ composition of rainfall; (ii) drip water average $\delta^{18}O$ composition from Fénix, located in Station LF, was 1-3‰ more negative than the annual amount-weighted $\delta^{18}O$ composition of rainfall, and; (iii) Station LF air relative humidity was at or near 100% during the entire recorded period (Y1-Y5). We know now that the observed positive composition of LF1 is not an artifact of the sampling protocol as previously proposed, because the new protocol confirms previous results. In this study, we provide new evidence that indicates that groundwater in Station LF may experience evaporation inside the chamber. However, the $\delta^{18}O$ and δD composition of LF1 and Fénix do not deviate markedly from the LMWL (Section 4.2.2 and LH19) suggesting that evaporation inside the chamber did not affect their isotopic compositions. Surface evaporation does not seem to influence Stations A and B drip sites, because they closely reflect the isotopic composition of rainfall (Y1, Y2, Y4). LF1 may have, however, a unique source routing configuration, perhaps receiving water from the overflow of a surface or shallow water pool exposed to evaporation, rather than reflecting direct infiltration, as the other drip sites.

For four consecutive years, Fénix, shows the most negative and stable isotopic composition of all drips. We support LH19's inference that this drip site reflects a large reservoir size preferentially incorporating large rainfall events with the lowest isotopic compositions, which typically happen during the summer rainy season (June-October). We recognize that a stalagmite $\delta^{18}O$ record reflecting the isotopic composition of such a drip site as Fénix, would tend to overestimate annual precipitation amount and be insensitive to drought, leading to underestimations of the magnitude of rapid precipitation reductions.

5.5. The transmission of the tropical cyclone signals

Rainfall associated with TCs is frequently distinguished by its characteristic depleted isotopic values relative to other tropical rainfall systems (Gedzelman et al. 2003). This is likely related to TC anatomy as their isotopic composition becomes more depleted towards their core (Gedzelman et al. 2003; Munksgaard et al. 2015). TC isotopic composition has been also related to their physical evolution, as well as their synoptic-scale meteorological setting; e.g. the proportion of convective to stratiform precipitation (Munksgaard et al. 2015; Aggarwal et al. 2016). As mentioned in Section 4.9, the amount of precipitation related to TCs characterized in this study does not explain their particularly depleted isotopic compositions. Therefore, under specific conditions described below, they may be distinguished as TC activity in a $\delta^{18}O$ stalagmite record from this location.

Clearly, the *Achilles heel* of TC detection in a stalagmite $\delta^{18}O$ record is not the stalagmite sampling resolution, since the sampling techniques are readily available

(Frappier et al. 2007a, 2007b), it lies in the relationship between the volume and isotopic composition of a drip water reservoir and the amount and isotopic composition of rainfall from a TC. At a single drip site, even TC with relatively weak precipitation amount and weak isotopic signal are expected to be more easily detected during times of persistent drought or when reservoirs are smaller and have a enriched isotopic composition. These conditions make the depleted TC isotopic signal to stand out from background, thus having a greater influence on the isotopic composition of drip water that can persist longer over time.

We examined our full five-year monitoring data in order to identify rainfall and drip water isotopic shifts associated with TCs (Figs. 6, 7 and 8). LF1 and B1 drip sites that have the shortest integration times reflect the largest isotopic response associated with the negative rainfall isotopic shifts of four TCs (Franklin, Alberto, Bill and Hannah, Figs. 6, 7 and 8, Supplementary Table D). On the other hand, Fénix and A7 drip sites, as expected from their long reservoir integration times, and negative isotopic compositions, reflected the weakest the influence of these TCs (Figs. 6, 7 and 8, Supplementary Table D). For future studies aimed at paleotempestology, stalagmites with small drip source reservoirs like LF1 are more sensitive to TC $\delta^{18}O$ signals than those with large reservoirs. Stalagmites with drip source reservoirs like Fénix with low $\delta^{18}O$ values and biased towards infiltration from heavy rainfall events, have poor isotopic contrast for TC detection, and are thus poor candidates for paleotempestology.

Lastly, as suggested by LH19 and shown in this study, the detection of TC rainfall fluxes is possible even when reservoir integration times vary from 3 to 15 months. How do we reconcile the observation of these relatively long residence times with the rapid isotopic shifts associated with TCs observed on weekly drip water samples? We can use our estimates of integration times to examine whether the observed negative shifts in drip water reflect the full mixing of TC rainfall with drip water reservoirs. Integration times provide the amount of rainfall (reservoir size in mm) that explains the $\delta^{18}O$ composition of drip sites prior to TC events. For this analysis, we examine TC Alberto ($\delta^{18}O = -6.9‰$, rainfall amount = 103 mm) because drip water and rainfall samples associated with this event were coeval, the event took place during a drought year with smaller epikarst water storage and greater rainfall $\delta^{18}O$ contrast, and the event is well represented by various drip water sites. We find that the expected drip water isotopic shifts from mixing TC Alberto rainfall with reservoir water from LF1, B1 and A3 is similar to the observed isotopic shifts (Supplementary material Table F). This suggests that even a weak TC with significant rainfall amount (~100 mm) and a sufficiently distinct negative isotopic signature relative to that of the reservoir prior to the event can be detected across drip reservoirs that integrate 3 to 15 months of rainfall accumulation. Furthermore, the magnitudes of drip water isotopic shifts associated with a TC are inversely related to reservoir integration times, as observed previously by Lases-Hernandez et al, (2019). This instrumental study supports that a low TC rainfall $\delta^{18}O$ signal impacts all drip locations to various extents, and that the magnitude and duration of the integrated $\delta^{18}O$ signal recorded in drip waters and stalagmite records will depend on epikarst reservoir hydrological characteristics, integrated hydroclimate, and sampling resolution, in agreement with Frappier (2013).

6. CONCLUSION

In Río Secreto cave, the observed $\delta^{18}O$ variability of five out of seven drip sites can be explained by integrating from 4 to 15 months of rainfall accumulation. Our integration approach explains not only the observed drip water $\delta^{18}O$ variability, but also closely approximates the absolute values. The isotopic composition of these five drip sites, with different reservoir sizes, converge into the same value after 15 months of drip water accumulation, reflecting the rainfall source and relatively fast residence times. Exceptions are Fénix, which reflects mostly wet season summer rainfall, and LF1, which closely matches the rainfall isotopic variability representing ~ 3 months of rainfall integration. LF1 annual average and amount-weighted $\delta^{18}O$ compositions are consistently more positive than the annual amount-weighted $\delta^{18}O$ composition of rainfall, due to evaporation processes above the cave. The observed residence times of reservoirs feeding drip sites in the Río Secreto cave system are relatively short compared to caves elsewhere.

Due mostly to epikarst reservoir size, agreement between coeval isotopic compositions of rainfall and drip water on an annual scale, does not necessarily reflect the assumption that drip water records coeval annual rainfall amount. In Río Secreto cave, drip sites show a tendency to best register the annual amount-weighted composition of rainfall and its interannual variability during typical rainfall years. Most drip sites fail to faithfully record a drought year (precipitation reduction by 50% from long-term average) when it follows a normal hydrological year but they are expected to approximate multiyear droughts more faithfully, as the isotopic inertia from the reservoir weakens. Speleothem $\delta^{18}O$-based proxy records would be therefore expected to underestimate the magnitude of intermittent annual droughts but probably properly characterize multi-year droughts.

We find evidence of the existence of an *amount effect* on interannual timescales in the YP in support of model results and therefore, reconstruction of precipitation variability from stalagmite $\delta^{18}O$ records on interannual timescales is possible in samples from the Río Secreto cave. As mentioned above, however, interannual rainfall reconstructions from stalagmite $\delta^{18}O$ records would not necessarily reflect the same time integration of rainfall amount; that is, annual stalagmite $\delta^{18}O$ values could represent over two years of rainfall amount depending on the drip water reservoir size.

This study shows that even within the same cave system, some drip sites may reflect the isotopic composition of rainfall quite accurately, while others may be biased by their drainage characteristics. We find one drip site biased towards the largest rainfall events while another is positively biased by evaporation processes. After integrating the amount of rainfall over the time, drip water results sug-

gest that a stalagmite from Río Secreto cave sampled at a monthly resolution may reflect from 3 to 15 months of rainfall accumulation, and sampled at an annual resolution, over 2 years of rainfall accumulation. Monitoring the isotopic composition of drip water is therefore important in order to characterize the extent to which the isotopic composition of drip water reflects rainfall, especially if studies aim at resolving seasonal and annual precipitation change.

In order for a stalagmite to capture individual tropical cyclones the following conditions are necessary: (1) drip water forming stalagmites must show weekly variability close to that of rainfall and stalagmite calcite or aragonite should be sampled at ~weekly resolution; (2) TCs must contribute with significant amount of rainfall relative to normal rainfall events preceding the TC, and with an isotopic signal sufficiently distinct from that of the reservoir. TC $\delta^{18}O$ signatures are retained in drip water, but after about a month, depending on the case, a new rainfall event large enough will dilute the TC signal. This is important because in the tropics when a study's goal is to characterize the isotopic signatures of TCs and/or hydroclimate extremes in general, drip water studies must be conducted at weekly resolution. A discrete sampling protocol is expected to approximate the amount-weighted isotopic composition of a drip, as long as it is conducted at a temporal resolution higher than the rainfall integration time by the drip reservoir (e.g. bi-weekly). This study complements the results from Lases-Hernandez et al. (2019) and highlights the importance of conducting multiyear monitoring of drip water and rainfall in order to interpret stalagmite $\delta^{18}O$ as a paleoclimate proxy

Declaration of Competing Interest

The authors declare that they have no known competing financial interests or personal relationships that could have appeared to influence the work reported in this paper.

ACKNOWLEDGEMENTS

We greatly appreciate the priceless support of the Río Secreto Natural Reserve family. Specially, we thank Tania Ramírez (Manager) and Otto Von Bertrab (Trustee) for their continuous interest in supporting and providing all the logistical aspects that have made this study and many others in Río Secreto, possible. We also specially thank the enthusiastic and knowledgable team of cave guides, photographers and staff members of Rio Secreto: to Lu Faccioli, Rodrigo Pimienta, Raúl Padilla, Alan Borjas, Isabel Barradas, Mely Ramos, Mónica Fernández, Jazmín Flores, Dan Venegas and Natalia Dixon. We also thank Peter Sprouse for providing Río Secreto Cave Map. We appreciate the revisions to this article by Dr. Juan Pablo Bernal, Dr. Patricia Beddows, associated editor Dr. Heather Stoll and two anonymous reviewers that help us to improve the clarity of this manuscript. We thank CONACYT-Mexico for providing a scholarship to support Fernanda Lases-Hernandez PhD studies at UNAM (Grant No. 440572), and the Waitt Grant #W457-16 that also offered support to her work in Río Secreto. This project was funded by NSF Grant # AGS-1702848.

APPENDIX A. SUPPLEMENTARY MATERIAL

Supplementary data to this article can be found online at https://doi.org/10.1016/j.gca.2020.07.008.

REFERENCES

Aggarwal P. K., Romatschke U., Araguas-Araguas L., Belachew D., Longstaffe F. J., Berg P., Schumacher C. and Funk A. (2016) Proportions of convective and stratiform precipitation revealed in water isotope ratios. *Nature Geosci.* **9**, 624–629.

Aharon P. and Dhungana R. (2017) Ocean-atmosphere interactions as drivers of mid-to-late Holocene rapid climate changes: Evidence from high-resolution stalagmite records at DeSoto Caverns, Southeast USA. *Quat. Sci. Rev.* **170**, 69–81.

Akers P. D., Brook G. A., Railsback L. B., Liang F., Iannon G., Webster J. W., Reeder P. P., Cheng H. and Edwards R. L. (2016) An extended and higher-resolution record of climate and land use from stalagmite MC01 from Macal Chasm, Belize, revealing connections between major dry events, overall climate variability, and Maya sociopolitical changes. *Palaeogeogr. Palaeoclimatol. Palaeoecol* **459**, 268–288.

Araguás-Araguás L., Froehlich K. and Rozanski K. (2000) Deuterium and oxygen-18 isotope composition of precipitation and atmospheric moisture. *Hydrol. Process.* **14**(8), 1341–1355.

Ayalon A., Bar-Matthews M. and Sass E. (1998) Rainfall-recharge relationships within a karstic terrain in the Eastern Mediterranean semi-arid region, Israel: $\delta^{18}O$ and dD characteristics. *J. Hydrol.* **207**, 18–31.

Baldini L. M., Baldini J. U. L., McElwaine J., Frappier A. B., Asmerom Y., Liu K. B., Prufer K., Ridley H. E., Polyak V., Kennett D. J., Macpherson C. G., Aquino V. V., Awe J. and Breitenbach S. F. M. (2016) Persistent northward North Atlantic tropical cyclone track migration over the past five centuries. *Sci. Rep.* **6**, 37522.

Bar-Matthews M. and Ayalon A. (2004) Speleothems as palaeoclimate indicators, a case study from Soreq Cave located in the Eastern Mediterranean Region, Israel. In *Past Climate Variability through Europe and Africa. Developments in Paleoenvironmental Research*, vol 6 (eds. R. W. Battarbee, F. Gasse and C. E. Stickley). Springer, Dordrecht, pp. 364–391.

Bauer-Gottwein P., Gondwe B. R., Charvet G., Marín L. E., Rebolledo-Vieyra M. and Merediz-Alonso G. (2011) the Yucatan Peninsula karst aquifer. *Mexico. Hydrogeol. J.* **19**, 507–524.

Beddows P. A., Mandic' M., Ford D. C. and Schwarcz H. P. (2016) Oxygen and hydrogen isotopic variations between adjacent drips in three caves at increasing elevation in a temperate coastal rainforest, Vancouver Island Canada. *Geochim. Cosmochim. Acta* **172**, 370–386.

Bradley C., Baker A., Jex C. N. and Leng M. J. (2010) Hydrological uncertainties in the modelling of cave drip-water $\delta^{18}O$ and the implications for stalagmite palaeoclimate reconstructions. *Quat. Sci. Rev.* **29**, 2201–2214.

Burns S. J., Fleitmann D., Matter A., Kramers J. and Al-Subbary A. A. (2003) Indian Ocean climate and an absolute chronology over Dansgaard/Oeschger events 9 to 13. *Science* **301**(5638), 1365–1367.

Clark I. D. and Fritz P. (1997) *Environmental Isotopes in Hydrogeology*. CRC/Lewis, New York, p. 328, ISBN: 9781566702492..

Cobb K. M., Adkins J. F., Partin J. W. and Clark B. (2007) Regional-scale climate influences on temporal variations of rainwater and cave dripwater oxygen isotopes in northern Borneo. *Earth Planet. Sci. Lett.* **263**, 207–220.

Craig H. (1961) Isotopic variations in meteoric waters. *Science* **133**, 1702–1703.

Cruz F. (2005) Stable isotope study of cave percolation waters in subtropical Brazil: implications for paleoclimate inferences from speleothems. *Chem. Geol.* **220**, 245–262.

Cuthbert M. O., Baker A., Jex C. N., Graham P. W., Treble P., Andersen M. S. and Acworth R. I. (2014) Drip water isotopes in semi-arid karst: implications for speleothem paleoclimatology. *Earth Planet. Sci. Lett.* **395**, 194–204.

Czuppon G., Demény A., Leél-Őssy S., Óvari M., Molnár M., Stieber J., Kiss K., Kármán K., Surányi G. and Haszpra L. (2018) Cave monitoring in the Béke and Baradla caves (Northeastern Hungary): implications for the conditions for the formation cave carbonates. *Int. J. Speleol.* **47**, 13–28.

Dansgaard W. (1964) Stable isotopes in precipitation. *Tellus* **16**, 436–468.

Déry S. J., Hernández-Henríquez M. A., Burford J. E. and Wood E. F. (2009) Observational evidence of an intensifying hydrological cycle in northern Canada. *Geophys. Res.* **36**, L13402. https://doi.org/10.1029/2009GL038852.

Douglas P. M., Pagani M., Canuto M. A., Brenner M., Hodell D. A., Eglinton T. I. and Curtis J. H. (2015) Drought, agricultural adaptation, and sociopolitical collapse in the Maya Lowlands. *Proc Natl Acad Sci.* **112**(18), 5607–5612.

Duan W., Ruan J., Luo W., Li T., Tian L., Zeng G., Zhang D., Bai Y., Li J., Tao T., Zhang P., Baker A. and Tan M. (2016) The transfer of seasonal isotopic variability between precipitation and drip water at eight caves in the monsoon regions of China. *Geochim. Cosmochim. Acta* **183**, 250–266.

Durack P. J., Wijffels S. E. and Matear R. J. (2012) Ocean salinities reveal strong global water cycle intensification during 1950 to 2000. *Science* **336**(6080), 455–458.

Fairchild I. and Treble P. (2009) Trace elements in speleothems as recorders of environmental change. *Quat. Sci. Rev.* **28**, 449–468.

Fairchild I. J., Tuckwell G. W., Baker A. and Tooth A. F. (2006) Modelling of dripwater hydrology and hydrogeochemistry in a weakly karstified aquifer (Bath, UK): implications for climate change studies. *J. Hydrol.* **321**, 213–231.

Fleitmann D., Cheng H., Badertscher S., Edwards R. L., Mudelsee M., Göktürk Ö. M., Fankhauser A., Pickering R., Raible C. C., Matter A., Kramers J. and Tüysüz O. (2009) Timing and climatic impact of Greenland interstadials recorded in stalagmites from northern Turkey. *Geophys Res Lett* **36**, L19707.

Frappier A. B., Sahagian D., Carpenter S. J., González L. A. and Frappier B. R. (2007a) Stalagmite stable isotope record of recent tropical cyclone events. *Geology* **35**, 111–114.

Frappier A., Knutson T., Liu K. B. and Emanuel K. (2007b) Perspective: coordinating paleoclimate research on tropical cyclones with hurricane-climate theory and modelling. *Tellus* **59**, 529–537.

Frappier A. B. (2013) Masking of interannual climate proxy signals by residual tropical cyclone rainwater: Evidence and challenges for low-latitude speleothem paleoclimatology. *Geochemi. Geophys. Geosyst.* **14**(9), 3632–3647.

Fuller L., Baker A., Fairchild I. J., Spötl C., Marca-Bell A., Rowe P. and Dennis P. F. (2008) Isotope hydrology of dripwaters in a Scottish cave and implications for stalagmite palaeoclimate research. *Hydrol. Earth Syst. Sci.* **12**, 1065–1074.

Gedzelman S., Hindman E. and Zhang X. (2003) Probing hurricanes with stable isotopes of rain and water vapor. *Mon. Wea. Rev.* **131**, 1112–1127.

Genty D. (2008) Palaeoclimate research in Villars Cave (Dordogne, SW-France). *Int. J. Speleol.* **37**, 173–191.

Genty D., Labuhn I., Hoffmann G., Danis P. A., Mestre O., Bourges F., Wainer K., Massault M., Van Exter S., Régnier E., Orengo P., Falourd S. and Minster B. (2014) Rainfall and cave water isotopic relationships in two South-France sites. *Geochim. Cosmochim. Acta.* **131**, 323–343.

Hartmann A. and Baker A. (2017) Modelling karst vadose zone hydrology and its relevance for paleoclimate reconstruction. *Earth-Sci. Rev.* **172**, 178–192.

Huntington H. G. (2006) A note on price asymmetry as induced technical change. *Energy J.* **27**(3), 1–7.

Jean-Baptiste P., Genty D., Fourré E. and Régnier E. (2019) Tritium dating of dripwater from Villars Cave (SW-France). *J. Appl.* **107**, 152–158.

Kao S. C. and Ganguly A. R. (2011) Intensity, duration, and frequency of precipitation extremes under 21st-century warming scenarios. *JGR-Atmospheres* **116**(D16).

Kaufman Aaro, Bar-Matthews Mirya, Ayalon Avne and Carmi Israe (2003) The vadose flow above Soreq Cave, Israel: a tritium study of the cave waters. *J. Hydrol.* **273**(1-4), 155–163 https://linkinghub.elsevier.com/retrieve/pii/S0022169402003943. https://doi.org/10.1016/S0022-1694(02)00394-3.

Kennett D. J., Breitenbach S. F., Aquino V. V., Asmerom Y., Awe J., Baldini J. U., Bartlein P., Culleton B. J., Ebert C. and Jazwa C. (2012) Development and disintegration of Maya political systems in response to climate change. *Science* **338**, 788–791.

Kluge T., Riechelmann D. F. C., Wieser M., Spotl C., Sultenfuss J., Schroder-Ritzrau A., Niggemann S. and Aeschbach-Hertig W. (2010) Dating cave drip water by tritium. *J. Hydrol.* **394**, 396–406.

Kurita N. (2013) Water isotopic variability in response to mesoscale convective system over the tropical ocean. *J. Geophys. Res. Atmos.* **118**(10), 376–10 390.

Lachniet M. S. and Patterson W. P. (2009) Oxygen isotope values of precipitation and surface waters in northern Central America (Belize and Guatemala) are dominated by temperature and amount effects. *Earth Planet. Sci. Lett.* **284**, 435–446.

Lachniet M. S., Asmerom Y., Polyak V. and Bernal J. P. (2017) Two millennia of Mesoamerican monsoon variability driven by Pacific and Atlantic synergistic forcing. *Quat. Sci. Rev.* **155**, 100–113.

Lachniet M. S., Bernal J. P., Asmerom Y., Polyak V. and Piperno D. (2012) A 2400-yr Mesoamerican rainfall history links climate and cultural change in Mexico. *Geology* **40**, 259–326.

Lases-Hernandez F., Medina-Elizalde M., Burns S. and DeCesare M. (2019) Long-term monitoring of drip water and groundwater stable isotopic variability in the Yucatán Peninsula: Implications for recharge and speleothem rainfall reconstruction. *Geochim. Cosmochim. Acta* **246**, 41–59.

Lu R. and Fu Y. (2010) Intensification of East Asian summer rainfall interannual variability in the twenty-first century simulated by 12 CMIP3 coupled models. *J. Clim.* **23**(12), 3316–3331.

Luo W., Wang S., Zeng G., Zhu X. and Liu W. (2014) Daily response of drip water isotopes to precipitation in Liangfeng Cave, Guizhou Province, SW China. *Quat. Int.* **349**, 153–158.

Magaña V., Amador J. A. and Medina S. (1999) The midsummer drought over Mexico and Central America. *J. Climate.* **12**, 1577–1588.

Maher B. A. and Thompson R. (2012) Oxygen isotopes from Chinese caves: records not of monsoon rainfall but of circulation regime. *J. Quat. Sci.* **27**(6), 615–624.

McDermott F. (2004) Palaeo-climate reconstruction from stable isotope variations in speleothems: a review. *Quat. Sci. Rev.* **23**, 901–918.

Medina-Elizalde M. and Rohling E. J. (2012) Collapse of Classic Maya civilization related to modest reduction in precipitation. *Science* **335**, 956–959.

Medina-Elizalde M., Burns S. J., Lea D. W., Asmerom Y., von Gunten L., Polyak V., Vuille M. and Karmalkar A. (2010) High

resolution stalagmite climate record from the Yucatán Peninsula spanning the Maya terminal classic period. *Earth Planet. Sci. Lett.* **298**, 255–262.

Medina-Elizalde M., Burns S. J., Polanco-Martínez J. M., Beach T., Lases-Hernández F., Shen C.-C. and Wang H.-C. (2016a) High-resolution speleothem record of precipitation from the Yucatán Peninsula spanning the Maya Preclassic Period. *Glob. Planet. Change* **138**, 93–102.

Medina-Elizalde M., Polanco-Martínez J. M., Lases-Hernández F., Bradley R. and Burns S. (2016b) Testing the "tropical storm" hypothesis of Yucatán Peninsula climate variability during the Maya Terminal Classic Period. *Quat. Res.* **86**, 111–119.

Medina-Elizalde M., Burns S. J., Polanco-Martinez J., Lases-Hernández F., Bradley R., Wang H.-C. and Shen C.-C. (2017) Synchronous precipitation reduction in the American Tropics associated with Heinrich 2. *Sci. Rep.* **7**, 11216.

Moerman J. W., Cobb K. M., Partin J. W., Meckler A. N., Carolin S. A., Adkins J. F., Lejau S., Malang J., Clark B. and Tuen A. A. (2014) Transformation of ENSO-related rainwater to dripwater $\delta^{18}O$ variability by vadose water mixing. *Geophys. Res. Lett.* **41**(22), 7907–7915.

Müller C., Cramer W., Hare W. L. and Lotze-Campen H. (2011). *Climate change risks for African agriculture* **108**, 4313–4315.

Munksgaard N. C., Zwart C., Kurita N., Bass A., Nott J. and Bird M. I. (2015) Stable isotope anatomy of tropical cyclone Ita, North-Eastern Australia, April 2014. *Plos One* **10** e0119728.

O'Gorman P. A. and Schneider T. (2009) The physical basis for increases in precipitation extremes in simulations of 21st-century climate change. *Proc. Natl Acad. Sci.* **106**(35), 14773–14777.

Onac B. P., Pace-Graczyk K. and Atudirei V. (2008) Stable isotope study of precipitation and cave drip water in Florida (USA): implications for speleothem-based paleoclimate studies. *Isot. Environ. Health Sci.* **44**, 149–161.

Partin J. W., Jenson J. W., Banner J. L., Quinn T. M., Taylor F. W., Sinclair D., Hardt B., Lander M. A., Bell T., Miklavič B., Jocson J. M. and Taboroši D. (2012) Relationship between modern rainfall variability, cave dripwater, and stalagmite geochemistry in Guam, USA. *Geochemi. Geophys. Geosyst.* **13** (3).

Pérez-Mejías C., Moreno A., Sancho C., Bartolomé M., Stoll H., Osácar M. C., Cacho I. and Delgado-Huertas A. (2018) Transference of isotopic signal from rainfall to dripwaters and farmed calcite in Mediterranean semi-arid karst. *Geochim. Cosmochim. Acta* **243**, 66–98.

Rao T. N., Radhakrishna B., Srivastava R., Satyanarayana T. M., Rao D. N. and Ramesh R. (2008) Inferring microphysical processes occurring in mesoscale convective systems from radar measurements and isotopic analysis *Geophys. Res. Lett.* **35**(9).

Risi C., Bony S. and Vimeux F. (2008) Influence of convective processes on the isotopic composition ($\delta^{18}O$ and δD) of precipitation and water vapor in the tropics: 2. Physical interpretation of the amount effect. *J. Geophys. Res. Atmos.* **113**(19), 148–227.

Riechelmann D. F. C., Schröder-Ritzrau A., Scholz D., Fohlmeister J., Spötl C., Richter D. K. and Mangini A. (2011) Monitoring Bunker Cave (NW Germany): a prerequisite to interpret geochemical proxy data of speleothems from this site. *J. Hydrol.* **409**, 682–695.

Riechelmann S., Schröder-Ritzrau A., Spötl C., Riechelmann D. F. C., Richter D. K., Mangini A., Frank N., Breitenbach S. F. M. and Immenhauser A. (2017) Sensitivity of Bunker Cave to climatic forcings highlighted through multi-annual monitoring of rain-, soil-, and dripwaters. *Chem. Geol.* **449**, 194–205.

Rozanski K., Araguas-Araguas L. and Gonfiantini R. (1993) Isotopic patterns in modern global precipitation. In *Climate Change in Continental Isotope Records* (eds. P.K. Swart, K.C. Lohman, J. McKenzie and S. Savin). *Am. Geophys. Union Monogr.* **78**, 1–36.

Seager R., Kushnir Y., Nakamura J., Ting M. and Naik N. (2010) Northern Hemisphere winter snow anomalies: ENSO, NAO and the winter of 2009/10. *Geophys. Res. Lett.* **37**, L14703. https://doi.org/10.1029/2010GL043830.

Sprouse P., Stan A., Ediger G., Graham K., Lloyd C., Moore D., Rincón J. (cartoonists). Addison A., Bordignon M., Bryant M., Burgos J., Cahun H., Alanis A., Ediger G., Ferreira A., Gouila C., Munguía M., Ramírez T., Rojo R., Solignac G., Sprouse P., Sprouse T, Vela G., Vela J., Von Bertrab O., Yañez G., Zabaleta M., Zappitello M., Zappitello S. and others (topographers) (2017) Map of the Pool Tunich System. Playa del Carmen, Quintana Roo, Mexico. Contact: peter@zaraenvironmental.com.

Treble P. C., Bradley C., Wood A., Baker A., Jex C. N., Fairchild I. J., Gagan M. K., Cowley J. and Azcurra C. (2013) An isotopic and modelling study of flow paths and storage in Quaternary calcarenite, SW Australia: implications for speleothem paleoclimate records. *Quat. Sci. Rev.* **64**, 90–103.

Vuille M., Bradley R. S., Healy R., Werner M., Hardy D. R., Thompson L. G. and Keimig F. (2003) Modeling $\delta^{18}O$ in precipitation over the tropical Americas: 2. Simulation of the stable isotope signal in Andean ice cores. *J. Geophys. Res.* **108**, 4175.

Wang X., Edwards R. L., Auler A. S., Cheng H., Kong X., Wang Y., Cruz F. W., Dorale J. A. and Chiang H. W. (2017) Hydroclimate changes across the Amazon lowlands over the past 45,000 years. *Nature* **541**, 204–207.

Wang Y. J., Cheng H., Edwards R. L., An Z. S., Wu J. Y., Shen C. C. and Dorale J. A. (2001) A high-resolution absolute-dated Late Pleistocene monsoon record from Hulu Cave, China. *Science* **294**(5550), 2345–2348.

Williams J. W., Jackson S. T. and Kutzbacht J. E. (2007) Projected distributions of novel and disappearing climates by 2100 AD. *Proc. Natl. Acad. Sci.* **104**, 5738–5742.

Williams P. P. W. and Fowler A. (2002) Relationship between oxygen isotopes in rainfall, cave percolation waters and speleothem calcite at Waitomo, New Zealand. *J. Hydrol. New. Zeal.* **41**, 53–70.

Wu T., Yu R., Zhang F., Wang Z., Dong M., Wang L., Xian J., Chen D. and Li L. (2010) The Beijing Climate Center atmospheric general circulation model: description and its performance for the present-day climate. *Clim. Dyn.* **34**(1), 123.

Yonge C., Ford D., Gray J. and Schwarcz H. (1985) Stable isotope studies of cave seepage water. *Chem. Geol.* **58**, 97–105.

Associate editor: Heather Stoll